

A Class of Higher-Order INAR Random Fields for Poisson Counts and Beyond

Christian H. Weiß^{a,*}, Angelika Silbernagel^{a,1}

^a*Department of Mathematics and Statistics, Helmut Schmidt University, Holstenhofweg 85, 22043 Hamburg, Germany.*

Abstract

Existing integer-valued autoregressive (INAR) models for count random fields suffer from difficulties in characterizing the stationary marginal distribution and in computing conditional probabilities (as required for likelihood inference). To overcome these drawbacks, the novel class of combined INAR (CINAR) models is proposed, which both exhibits the classical autoregressive dependence structure and allows to specify the marginal distribution within the wide class of discrete self-decomposable distributions. In particular, CINAR random fields can be equipped with a Poisson or negative-binomial marginal distribution. The CINAR's key stochastic properties are derived (including a simple expression for conditional probabilities), and special cases as well as possible extensions are discussed. Approaches for parameter estimation are developed and investigated, and the practical relevance of the novel CINAR family is demonstrated by an agricultural data application.

Keywords: Autocorrelation function, Autoregressive model, Count data, Discrete self-decomposable distributions, Random field, Spatial dependence

2020 MSC: Primary 60G60, 62M40 Secondary 60G10, 62M10

1. Introduction

In many applications, we are concerned with data that are located on a regular two-dimensional grid; the corresponding data-generating process (DGP) is commonly referred to as a random field. Such grid data and random fields can be understood as “plane extensions” of time series and stochastic processes, respectively. Hence, it is not surprising that many models for random fields arise from analogous time-series models. In the case of continuously distributed random fields, for example, the random-field versions of the classical autoregressive (AR) and moving-average (MA) models as developed by Whittle (1954); Besag (1974); Haining (1978); Basu and Reinsel (1993) are often used in applications. In the present research, however, we are concerned with a different type of random fields, namely count random fields $(X_{s,t}) = (X_{s,t})_{s,t \in \mathbb{Z} = \{\dots, -1, 0, 1, \dots\}}$ having $\mathbb{N}_0 = \{0, 1, \dots\}$ as their range. Corresponding applications with count grid data can be found in various fields of practice, such as agriculture (Tabandeh and Ghodsi, 2024), biology (Chutoo et al., 2021), or epidemiology (Yang et al., 2025). As with continuously distributed random fields, it makes sense to adapt established models from the field of count time series to the case of count random fields. In the seminal article by Ghodsi et al. (2012), a spatial analog of the famous first-order integer-valued AR (INAR(1)) model known from count time series analysis (see Weiß, 2018 for a comprehensive survey) was introduced, which the authors originally referred to as the “first-order spatial INAR (SINAR(1, 1))” model. In what follows, however, we use the terminology of Silbernagel and Weiß (2026a) who refer to this model as the INAR(1, 1) *random field*, as this notion emphasizes the grid structure of the data and avoids confusion with other types of spatial count data (for the latter, see Glaser (2017); Jung and Glaser (2022) and the references therein). The (unilateral) INAR(1, 1) random field is defined by the recursion

$$X_{s,t} = \alpha_{01} \circ X_{s,t-1} + \alpha_{10} \circ X_{s-1,t} + \alpha_{11} \circ X_{s-1,t-1} + \varepsilon_{s,t}, \quad (1)$$

*Corresponding author. ORCID: 0000-0001-8739-6631.

Email addresses: weissc@hsu-hh.de (Christian H. Weiß), silbernagel@hsu-hh.de (Angelika Silbernagel)

¹ORCID: 0009-0002-6993-244X.

where the model's dependence parameters satisfy

$$\alpha_{01}, \alpha_{10}, \alpha_{11} \in [0, 1) \quad \text{and} \quad \alpha_{01} + \alpha_{10} + \alpha_{11} < 1, \quad (2)$$

and where the count innovations $(\varepsilon_{s,t}) = (\varepsilon_{s,t})_{s,t \in \mathbb{Z}}$ are independent and identically distributed (i.i.d.) with mean $\mu_\varepsilon > 0$ and variance $\sigma_\varepsilon^2 > 0$. Moreover, introducing the short-hand notation $\mathcal{P}_{s,t} = \{X_{s-k,t-l} : k \geq 1 \text{ or } l \geq 1\}$ for the “past” corresponding to “time” (s, t) (note the “or” in the definition of $\mathcal{P}_{s,t}$), the innovation $\varepsilon_{s,t}$ at “time” (s, t) is assumed to be independent of $\mathcal{P}_{s,t}$ for all $s, t \in \mathbb{Z}$. Finally, the operation “ \circ ” in (1) refers to the so-called “binomial thinning operator”, which serves as an integer substitute of the ordinary multiplication (Weiß, 2008a). For a discrete count random variable X with range \mathbb{N}_0 and a constant $\alpha \in (0, 1)$, it is defined by $\alpha \circ X := \sum_{i=1}^X Z_i$ (together with the convention that empty sums are equal to zero), where the counting series $(Z_i)_{i \in \mathbb{N}=\{1,2,\dots\}}$ is a sequence of i.i.d. Bernoulli random variables with $\mathbb{P}(Z_i = 1) = \alpha$, which is independent of X . The boundary values $\alpha \in \{0, 1\}$ can be included by the conventions $0 \circ X := 0$ and $1 \circ X := X$. The thinnings at point (s, t) appearing in (1) are assumed to be performed independently of each other, to be independent of $(\varepsilon_{i,j})$, and, see Silbernagel and Weiß (2026a) for a discussion, to be independent of $\mathcal{P}_{s,t}$ as well.

The INAR(1, 1) random field (1) of Ghodsi et al. (2012) has been studied and modified in many subsequent works, see Ghodsi (2015); Chutoo et al. (2021); Sassi and Paraíba (2023); Ghodsi et al. (2024); Karlis et al. (2024); Tabandeh and Ghodsi (2024); Ghodsi and Bakouch (2025); Yang et al. (2025); Silbernagel and Weiß (2026a) for details. Moreover, Silbernagel and Weiß (2026a) extended the INAR(1, 1) model to higher-order autoregressions, namely to the INAR(p_1, p_2) model of order $(p_1, p_2) \in \mathbb{N}^2$ being defined by the recursion

$$X_{s,t} = \sum_{(i,j) \in \mathcal{S}} \alpha_{ij} \circ X_{s-i,t-j} + \varepsilon_{s,t} \quad \text{with } \mathcal{S} := \{(i, j) \mid 0 \leq i \leq p_1, 0 \leq j \leq p_2, (i, j) \neq (0, 0)\}, \quad (3)$$

and derived its key stochastic properties. However, these “default” INAR models for count random fields, as defined in the aforementioned references, have the drawback that closed-form expressions for the stationary marginal distribution are difficult to obtain. This problem is caused by the multiple thinnings at each point (s, t) , and it is already evident in the first-order case $p_1 = p_2 = 1$, recall (1). For example, it is not clear how spatially dependent Poisson (Poi) counts could be obtained by an INAR random field, i.e., how the innovations' distribution has to be chosen such that the generated $X_{s,t}$ are Poi-distributed (if possible at all). This differs from the time-series case, where at least the INAR(1) model can be equipped with a Poi-marginal distribution (and some further common distributions, see Section 2.1 for details). Up to now, the only ARMA-like approach for Poi-grid data appears to be the integer-valued MA (INMA) random field of Silbernagel and Weiß (2026b), which can be equipped with a Poi-marginal distribution for any model order. On the other hand, MA-type models have a memory that ends abruptly, whereas the memory of AR-type models fades out gradually and, thus, often better matches real-world data. Therefore, it would be attractive for practice to have an INAR-type model for count random fields that allows for a Poi-marginal distribution (or other common distributions) at the same time.

The drawback of having an unclear marginal distribution is also well known from the INAR(p) time-series model with $p > 1$ according to Du and Li (1991) (whereas the Poi-INAR(p) model of Alzaid and Al-Osh (1990) does not exhibit the typical AR(p) autocorrelation structure). A possible solution that combines both an AR(p)-like autocorrelation function (ACF) and a Poi-marginal distribution was developed by Weiß (2008b) based on preliminary work by Zhu and Joe (2006). Their idea was to combine the INAR(1) time-series model (involving only one thinning per time) with a random-selection mechanism, with the resulting models being referred to as *combined INAR (CINAR) models*. In what follows, we adapt this idea to the case of count random fields by developing the novel class of CINAR random fields, see Section 2. There, we also derive the key stochastic properties of the proposed (unilateral) CINAR family, discuss important special cases, and present possible future extensions. Section 3 develops possible approaches for the parameter estimation of CINAR models, the finite-sample performances of which are investigated in Section 4 by a comprehensive simulation study. The practical relevance of the novel CINAR class is demonstrated in Section 5, where a real-world data application from an agricultural experiment is presented. Finally, we conclude in Section 6 and outline directions for future research.

2. The Combined INAR Random Field

Inspired by the works of Zhu and Joe (2006); Weiß (2008b) on count time series, let us propose the class of combined INAR models for count random fields.

Definition 2.0.1. Like in (3), let $\mathcal{S} := \{(i, j) \mid 0 \leq i \leq p_1, 0 \leq j \leq p_2, (i, j) \neq (0, 0)\}$ for given $p_1, p_2 \in \mathbb{N}$. We say that the random field $(X_{s,t})_{s,t \in \mathbb{Z}}$ follows a (unilateral) *CINAR*(p_1, p_2) *model* if it satisfies the recursion

$$X_{s,t} = \sum_{(i,j) \in \mathcal{S}} D_{s,t;i,j} \cdot (\alpha \circ X_{s-i,t-j}) + \varepsilon_{s,t}, \quad (4)$$

where

- $(\varepsilon_{s,t})$ are i.i.d. count innovations and $\alpha \in (0, 1)$ is a constant;
- $(\mathbf{D}_{s,t})_{s,t \in \mathbb{Z}}$ is an i.i.d. random field of $|\mathcal{S}|$ -dimensional “decision” random vectors $\mathbf{D}_{s,t} = (D_{s,t;0,1}, \dots, D_{s,t;p_1,p_2})$ that follow the multinomial distribution $\text{MULT}(1; \phi_{01}, \dots, \phi_{p_1 p_2})$ with probabilities ϕ_{ij} satisfying $\sum_{(i,j) \in \mathcal{S}} \phi_{ij} = 1$ (i.e., where exactly one of the $|\mathcal{S}|$ components takes the value 1 and all others equal 0), which are also independent of the innovations $(\varepsilon_{s,t})$;
- $\varepsilon_{s,t}$ and $\mathbf{D}_{s,t}$ are independent of the “past” $\mathcal{P}_{s,t}$;
- the thinnings at “time” (s, t) are performed independently of each other, of $(\varepsilon_{s,t})$, $(\mathbf{D}_{s,t})$, and the “past” $\mathcal{P}_{s,t}$.

If useful for a detailed understanding, we shall also add the subscript “ s, t ” to the thinnings in (4) in order to emphasize that the thinnings are executed at point (s, t) and are not identical to thinnings being executed at other locations. The recursion (4) in Definition 2.0.1 states that $X_{s,t}$ is equal to $\alpha \circ X_{s-i,t-j} + \varepsilon_{s,t}$ with probability $\phi_{i,j}$, for $(i, j) \in \mathcal{S}$. Hence, by contrast to the ordinary *INAR*(p_1, p_2) recursion (3), the *CINAR*(p_1, p_2) random field uses only one thinning operator at each location (s, t) , which shall later allow us to conclude on its stationary marginal distribution, see Section 2.1 for details.

Remark 2.0.2. Comparing Definition 2.0.1 with the corresponding definition of the *CINAR* time-series model in Weiß (2008b), we note slightly different assumptions on the joint distribution of the involved thinnings. The *CINAR* random-field model is defined by assuming that the thinnings at “time” (s, t) are performed independently of the “past” $\mathcal{P}_{s,t}$, whereas the *CINAR* time-series model would correspond to assuming the thinnings *being applied to* $X_{s,t}$ (at “later times”) to be independent of the “past” $\mathcal{P}_{s,t}$. In the latter setup, different assumptions on the joint distribution of the thinnings would be possible, which would then lead to different model types in analogy to Weiß (2008b). The former setup (the one chosen by us in Definition 2.0.1), by contrast, is analogous to the “independent thinnings” approach in Weiß (2008b), and it has also been considered by Silbernagel and Weiß (2026a) in the context of ordinary *INAR* random fields. Here, we adapt the approach of Silbernagel and Weiß (2026a) to ensure the tractability of the model properties as well as the comparability between *INAR* and *CINAR* models for count random fields. We refer the reader to Silbernagel and Weiß (2026a, Remark 2) for a more detailed discussion.

2.1. Stochastic Properties of *CINAR* Random Fields

Let us start our investigations with a general result on the ergodicity of *CINAR* random fields.

Proposition 2.1.1. *A stationary CINAR random field according to Definition 2.0.1 is ergodic.*

The proof of Proposition 2.1.1, which is presented in Appendix A.1, employs standard techniques in analogy to, e.g., the corresponding proof of Ghodsi (2015) for the *INAR*(1, 1) random field.

While the definition in (4) might look somewhat artificial at first glance, its main advantage becomes clear with the following result on the stationary marginal distribution of $(X_{s,t})$. There, the marginal distribution is expressed in terms of the probability generating function (pgf) of $X_{s,t}$, i.e., of $\text{pgf}_X(u) = \mathbb{E}(u^{X_{s,t}})$, which uniquely encodes the probability mass function (PMF) of $X_{s,t}$.

Proposition 2.1.2. *Let $(X_{s,t})$ be a stationary CINAR random field according to Definition 2.0.1. Then, its marginal distribution satisfies*

$$\text{pgf}_X(u) = \text{pgf}_X(1 - \alpha + \alpha u) \cdot \text{pgf}_\varepsilon(u), \quad (5)$$

where mean and variance are given by

$$\mu_X = \frac{\mu_\varepsilon}{1 - \alpha} \quad \text{and} \quad \sigma_X^2 = \frac{\alpha \mu_\varepsilon + \sigma_\varepsilon^2}{1 - \alpha^2} = \mu_X \frac{\alpha + \sigma_\varepsilon^2 / \mu_\varepsilon}{1 + \alpha}, \quad \text{respectively.} \quad (6)$$

The proof of Proposition 2.1.2 is presented in Appendix A.2. Note that (5) corresponds to the pgf recursion of the classical INAR(1) model, i.e., the CINAR(p_1, p_2) model can be equipped with exactly those marginal distributions that can also be attained by the classical INAR(1) model (Weiß, 2018, Section 2.1.3). In particular, in analogy to the INMA random field discussed in Silbernagel and Weiß (2026b), compound Poisson (CP)-distributed innovations $\varepsilon_{s,t}$ lead to CP-distributed observations $X_{s,t}$. Furthermore, we can choose each member of the family of discrete self-decomposable (DSD) distributions as a marginal distribution of $X_{s,t}$, where the required innovations' distribution is then given by $\text{pgf}_\varepsilon(u) = \text{pgf}_X(u) / \text{pgf}_X(1 - \alpha + \alpha u)$. The DSD family includes, among others, the Poi- and negative-binomial (NB) distribution (see Zhu and Joe (2003); Weiß (2008a) as well as Example 2.2.1 below for further details), which are also later considered in our simulation study presented in Section 4. Equation (6), in turn, shows that we have over-/equi-/underdispersed observations if and only if (iff) the innovations are over-/equi-/underdispersed.

Next, we investigate the spatial dependence structure of the stationary CINAR random field $(X_{s,t})$. For $k, l \in \mathbb{Z}$, its spatial ACF ρ is defined by

$$\rho(k, l) = \text{Corr}(X_{s,t}, X_{s+k, t+l}) = \frac{\text{Cov}(X_{s,t}, X_{s+k, t+l})}{\mathbb{V}(X_{s,t})}.$$

Note that $\rho(k, l) = \rho(-k, -l)$ by definition. As shown in the following proposition, the CINAR's ACF satisfies a set of Yule–Walker (YW) equations.

Proposition 2.1.3. *Let $(X_{s,t})$ be a stationary CINAR random field according to Definition 2.0.1. Then, its ACF satisfies the recursions*

$$\rho(k, l) = \alpha \sum_{(i,j) \in \mathcal{S}} \phi_{ij} \rho(k - i, l - j) \quad \text{if } k \geq 1 \text{ or } l \geq 1, \quad (7)$$

$$\rho(k, l) = \alpha \sum_{(i,j) \in \mathcal{S}} \phi_{ij} \rho(k + i, l + j) \quad \text{if } k \leq -1 \text{ or } l \leq -1. \quad (8)$$

The proof of Proposition 2.1.3 is presented in Appendix A.3. Note that Equation (7) holds in the region illustrated by Figure 1 (b), and Equation (8) in the one of Figure 1 (c). Also note that the YW equations of Proposition 2.1.3 agree with those of the ordinary INAR(p_1, p_2) random field after the following reparametrization: if one defines $\theta_{ij} = \alpha \cdot \phi_{ij}$ with $\sum_{(i,j) \in \mathcal{S}} \theta_{ij} = \alpha$, then the θ_{ij} are the counterparts to the AR coefficients α_{ij} in (3). In particular, replacing θ_{ij} in Proposition 2.1.3 by α_{ij} , we obtain Proposition 5 of Silbernagel and Weiß (2026a). Hence, altogether, the CINAR(p_1, p_2) approach combines two highly attractive features, namely the classical AR-type autocorrelation structure with a broad variety of possible marginal distributions. So recalling George Box' famous words "All models are wrong, but some are useful", we clearly judge the CINAR models as being useful for practice despite their somewhat technical definition.

A further advantage of the CINAR compared to the ordinary INAR approach becomes clear when studying its regression properties.

Proposition 2.1.4. *Let $(X_{s,t})$ be a stationary CINAR random field according to Definition 2.0.1. Then, the conditional distribution is given by*

$$\mathbb{P}(X_{s,t} = x | \mathcal{P}_{s,t}) = \sum_{y=0}^x \mathbb{P}(\varepsilon_{s,t} = y) \cdot \sum_{(i,j) \in \mathcal{S}} \phi_{ij} \cdot \binom{X_{s-i, t-j}}{x-y} \alpha^{x-y} (1 - \alpha)^{X_{s-i, t-j} - x + y}, \quad (9)$$

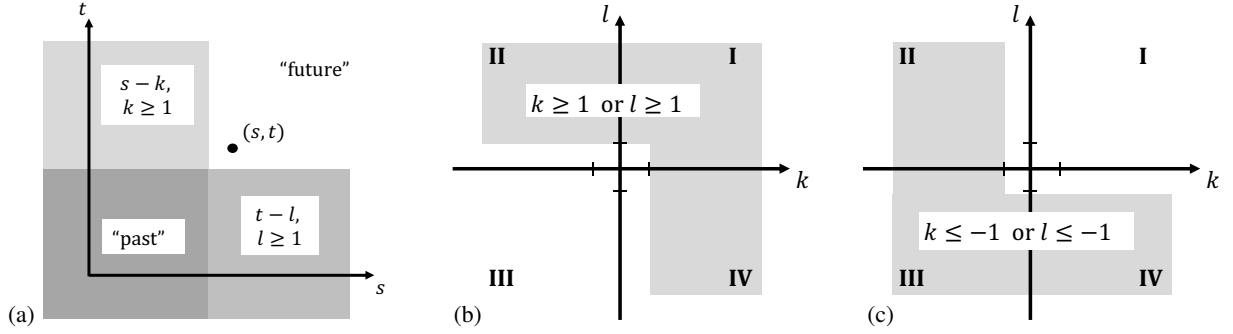


Fig. 1: (a) Process' "past" corresponding to "time" (s, t) . Spatial lags (k, l) and Quadrants I-IV, where (b) equation (7) or (c) equation (8) holds. Graphs adapted from Silbernagel and Weiß (2026a, Fig. 1)

where the binomial probabilities $\binom{X_{s-i,t-j}}{x-y} \alpha^{x-y} (1-\alpha)^{X_{s-i,t-j}-x+y}$ are equal to zero if $x - y > X_{s-i,t-j}$. In particular, the conditional mean and variance are given by

$$\mathbb{E}(X_{s,t} | \mathcal{P}_{s,t}) = \mu_\varepsilon + \alpha \sum_{(i,j) \in \mathcal{S}} \phi_{ij} X_{s-i,t-j} \quad (10)$$

and

$$\mathbb{V}(X_{s,t} | \mathcal{P}_{s,t}) = \sigma_\varepsilon^2 + \alpha(1-\alpha) \sum_{(i,j) \in \mathcal{S}} \phi_{ij} X_{s-i,t-j} + \alpha^2 \sum_{(i,j) \in \mathcal{S}} \phi_{ij} X_{s-i,t-j}^2 - \alpha^2 \sum_{(i,j),(k,l) \in \mathcal{S}} \phi_{ij} \phi_{kl} X_{s-i,t-j} X_{s-k,t-l}, \quad (11)$$

respectively.

The proof of Proposition 2.1.4 is presented in Appendix A.4. Note that Proposition 2.1.4 is of utmost importance for statistical inference. First, it can be utilized for parameter estimation, namely the conditional mean (10) for conditional least squares (CLS) estimation and the conditional distribution (9) for conditional maximum likelihood (CML) estimation, see Section 3 for details. Secondly, Proposition 2.1.4 is useful for model diagnostics, as it allows to compute the standardized Pearson residuals and the probability integral transform (PIT) histogram, see Weiß (2018, Section 2.4) and Jung and Glaser (2022) for details. These diagnostic tools shall also later be used in our data application presented in Section 5.

As mentioned before, Proposition 2.1.4 shows a further major advantage of the CINAR compared to the INAR approach: the conditional probabilities (9) are much simpler to compute than those of classical INAR random fields, as we are only concerned with one convolution as caused by the single selected binomial thinning at location (s, t) . By contrast, the INAR(1, 1) random field requires a three-fold convolution (see Ghodsi, 2015, Proposition 2.1), and the INAR(p_1, p_2) random field more generally an $|\mathcal{S}|$ -fold convolution (see Silbernagel and Weiß, 2026a, Proposition 7). Also the multilateral INAR(1, 1) model according to Karlis et al. (2024) is computationally much more demanding, as it requires an eight-fold convolution according to their Equation (9). Note that a brief discussion on multilateral CINAR models is provided in Section 2.3 below. But first, let us take a closer look at the case of the first-order CINAR model.

2.2. Special Case: The CINAR(1, 1) Model

Up to now, the vast majority of articles on count random fields focused on the first-order INAR model, i.e., on model (1) and its modifications, recall the literature review in Section 1. In fact, this special case often turned out to be sufficient for modeling real-world count grid data, and it was also possible to derive closed-form expressions for its spatial ACF. However, as already mentioned, even for these first-order INAR models like (1), it was not possible to characterize the stationary marginal distribution beyond expressions for mean and variance. Therefore, the present section presents a brief overview on essential stochastic properties of the CINAR(1, 1) model, defined by the recursion

$$X_{s,t} = D_{s,t;0,1}(\alpha \circ X_{s,t-1}) + D_{s,t;1,0}(\alpha \circ X_{s-1,t}) + D_{s,t;1,1}(\alpha \circ X_{s-1,t-1}) + \varepsilon_{s,t}, \quad (12)$$

as a natural competitor to the existing INAR(1, 1) models. The corresponding marginal distribution is characterized in Proposition 2.1.2, which applies to CINAR models of any order in the same way. In particular, as for any model order (p_1, p_2) , it is possible to achieve Poi- or NB-distributed outcomes $X_{s,t}$.

Example 2.2.1. If the innovations $(\varepsilon_{s,t})$ of a CINAR random field (of any order) are i.i.d. Poi-distributed according to $\text{Poi}(\mu_\varepsilon)$, then the observations $X_{s,t}$ are Poi-distributed as well (and thus equidispersed, i.e., $\sigma_X^2 = \mu_X$), namely $X_{s,t} \sim \text{Poi}(\mu_X)$ with $\mu_X = \mu_\varepsilon / (1 - \alpha)$, see Weiß (2008a, Example 3.3). We refer to this special case as the Poi-CINAR model.

If, by contrast, we want to achieve the (overdispersed) NB-distribution for $X_{s,t}$, say, $X_{s,t} \sim \text{NB}(\nu, \pi)$ with $\nu > 0$ and $\pi \in (0, 1)$ such that $\mu_X = \nu(1 - \pi)/\pi$ and $\sigma_X^2/\mu_X = 1/\pi > 1$, then the innovations must have the following PMF (Weiß, 2008a, Example 3.4):

$$P(\varepsilon_{s,t} = k) = \begin{cases} (1 - (1 - \pi)(1 - \alpha))^\nu & \text{if } k = 0, \\ \sum_{j=1}^k \binom{\nu}{j} (1 - (1 - \pi)(1 - \alpha))^{\nu-j} ((1 - \pi)(1 - \alpha))^j \cdot \binom{k-1}{k-j} (1 - \pi)^{k-j} \pi^j & \text{if } k > 0, \end{cases}$$

where the (generalized) binomial coefficient $\binom{\nu}{j}$ is defined by $\Gamma(\nu + 1) / (\Gamma(\nu - j + 1) \cdot j!)$. The mean and variance of $\varepsilon_{s,t}$ satisfy the equations given in Proposition 2.1.2, and we refer to the model as the NB-CINAR one.

Propositions 2.1.3 and 2.1.4 simplify for the CINAR(1, 1) model by using that $\mathcal{S} = \{(0, 1), (1, 0), (1, 1)\}$. Since the YW equations of Proposition 2.1.3 agree with those of the stationary INAR(p_1, p_2) random field (3) after replacing $\theta_{ij} = \alpha \phi_{ij}$ by α_{ij} (see Silbernagel and Weiß, 2026a, Proposition 5), we also obtain the same solution in the special case $p_1 = p_2 = 1$ as for the ordinary INAR(1, 1) random field, i.e., the same closed-form expression for the ACF. This expression is provided by Proposition 3.2 of Ghodsi et al. (2012) as well as Proposition 2 and Corollary 1 of Silbernagel and Weiß (2026a), and it remains valid after replacing their α_{ij} by our θ_{ij} , which leads to the following corollary.

Corollary 2.2.2. *Let $(X_{s,t})$ be a stationary CINAR(1, 1) random field according to Definition 2.0.1 and Equation (12), let $k, l \geq 0$. Then, the ACF over Quadrants II and IV (recall Figure 1) is given by*

$$\rho(-k, l) = \rho(k, -l) = \lambda^k \eta^l \quad \text{with } \lambda, \eta \in (0, 1),$$

where

$$\lambda = \frac{1 + \alpha^2(\phi_{10}^2 - \phi_{01}^2 - \phi_{11}^2) - \sqrt{(1 + \alpha^2(\phi_{10}^2 - \phi_{01}^2 - \phi_{11}^2))^2 - 4\alpha(\phi_{10} + \alpha\phi_{01}\phi_{11})}}{2\alpha(\phi_{10} + \alpha\phi_{01}\phi_{11})} \quad \text{and} \quad \eta = \frac{\alpha(\phi_{01} + \phi_{11}\lambda)}{1 - \alpha\phi_{10}\lambda}.$$

Furthermore, the ACF over Quadrants I and III, $\rho(-k, -l) = \rho(k, l)$, satisfies $\rho(k, 0) = \lambda^k$, $\rho(0, l) = \eta^l$, and

$$\rho(k, l) = \alpha\phi_{01}\rho(k, l-1) + \alpha\phi_{10}\rho(k-1, l) + \alpha\phi_{11}\rho(k-1, l-1) \quad \text{for } k, l \geq 1.$$

To sum up, the CINAR(1, 1) random field exhibits the same autocorrelation structure as existing INAR(1, 1) random fields, but it can be easily equipped with common marginal distributions, and also its conditional probabilities are simpler to compute. Thus, the CINAR(1, 1) model is an appealing competitor of existing INAR(1, 1) models for count random fields.

2.3. Outlook on Possible Extensions

Let us conclude Section 2 by briefly discussing possible future extensions of our novel CINAR(p_1, p_2) model for count random fields. First, in analogy to the multilateral INAR(1, 1, 1, 1) model of Karlis et al. (2024), one could define a multilateral CINAR recursion of order $(p_1, p_2, q_1, q_2) \in \mathbb{N}^4$ as

$$X_{s,t} = \sum_{(i,j) \in \mathcal{S}^*} D_{s,t;i,j} \cdot (\alpha \circ X_{s-i,t-j}) + \varepsilon_{s,t} \quad (13)$$

similar to Definition 2.0.1, where $\mathcal{S}^* := \{(i, j) \mid -q_1 \leq i \leq p_1, -q_2 \leq j \leq p_2, (i, j) \neq (0, 0)\}$, and where the ‘‘past’’ $\mathcal{P}_{s,t}$ is replaced by $\mathcal{A}_{s,t} = \{X_{u,v} : (u, v) \neq (s, t)\}$, i.e., all random variables other than $X_{s,t}$. Then, the marginal properties according to Proposition 2.1.2 could be shown to hold for the multilateral CINAR(p_1, p_2, q_1, q_2) recursion as well by simply replacing the summation across \mathcal{S} in the proof in Appendix A.1 by a summation across \mathcal{S}^* . In a similar way, the conditional probability (9) in Proposition 2.1.4 would change to

$$\mathbb{P}(X_{s,t} = x \mid \mathcal{A}_{s,t}) = \sum_{y=0}^x \mathbb{P}(\varepsilon_{s,t} = y) \cdot \sum_{(i,j) \in \mathcal{S}^*} \phi_{ij} \cdot \binom{X_{s-i,t-j}}{x-y} \alpha^{x-y} (1-\alpha)^{X_{s-i,t-j}-x+y}, \quad (14)$$

which again involves only a single convolution. Formula (14) is computationally much cheaper than Equation (9) in Karlis et al. (2024), because their conditional probability involves an eight-fold convolution instead. While a comprehensive analysis of its stochastic properties is certainly still pending (in particular, parameter estimation is expected to be demanding in view of Whittle, 1954), the above illustrations already indicate that a multilateral CINAR model defined via (13) could become an appealing competitor of the multilateral INAR model developed by Karlis et al. (2024). Thus, a detailed investigation of a multilateral CINAR model is recommended for future research.

Second, one could extend the CINAR random field to negative dependencies by combining it with the Tobit approach developed by Weiß et al. (2026) in the time-series case. More precisely, with the same assumptions as in Definition 2.0.1, the Tobit CINAR(p_1, p_2) model for count random fields would be defined by

$$X_{u,v} = \max\{0, Y_{u,v}\} \quad \text{with} \quad Y_{u,v} = \sum_{(i,j) \in \mathcal{S}} D_{u,v;i,j} \cdot s(i, j) \cdot (\alpha \circ X_{u-i,v-j}) + \varepsilon_{u,v}, \quad (15)$$

where $s(i, j) \in \{\pm 1\}$ denotes the specified sign of the $(i, j)^{\text{th}}$ autoregressive term. Here, the censoring at zero avoids that $X_{u,v}$ becomes negative, whereas $Y_{u,v}$ is allowed to do so. For example, a Tobit CINAR(1, 1) model might be defined by

$$X_{u,v} = \max\{0, Y_{u,v}\} \quad \text{with} \quad Y_{u,v} = D_{u,v;0,1} \cdot (\alpha \circ X_{u,v-1}) + D_{u,v;1,0} \cdot (\alpha \circ X_{u-1,v}) - D_{u,v;1,1} \cdot (\alpha \circ X_{u-1,v-1}) + \varepsilon_{u,v}$$

if one chooses $s(0, 1) = s(1, 0) = +1$ and $s(1, 1) = -1$. For the general Tobit CINAR(p_1, p_2) model (15), the conditional distribution $\mathbb{P}(X_{u,v} = x \mid \mathcal{P}_{u,v})$ is computed in two steps. Abbreviate the PMF of the Bin(n, π)-distribution by $\mathfrak{p}_{n,\pi}(z)$ for $z \in \mathbb{Z}$, which equals zero if $z \notin \{0, \dots, n\}$. Then,

$$\mathbb{P}(Y_{u,v} = x \mid \mathcal{P}_{u,v}) = \sum_{(i,j) \in \mathcal{S}} \phi_{ij} \cdot \sum_{y=0}^{\infty} \mathbb{P}(\varepsilon_{u,v} = y) \cdot \mathfrak{p}_{X_{u-i,v-j}, \alpha}(s(i, j) \cdot (x - y)) \quad \text{for } x \in \mathbb{Z}, \quad (16)$$

where for each $(i, j) \in \mathcal{S}$, the inner summation across y has only finitely many non-zero summands due to the finite support of $\mathfrak{p}_{X_{u-i,v-j}, \alpha}(z)$. For the same reason, there always exists a finite lower bound $L_{u,v}$ for the support of $\mathbb{P}(Y_{u,v} = x \mid \mathcal{P}_{u,v})$, namely $L_{u,v} := \sum_{(i,j) \in \mathcal{S}} \min\{0, s(i, j)\} \cdot X_{u-i,v-j}$. Then,

$$\mathbb{P}(X_{u,v} = x \mid \mathcal{P}_{u,v}) = \begin{cases} \mathbb{P}(Y_{u,v} = x \mid \mathcal{P}_{u,v}) & \text{if } x > 0, \\ \sum_{z=L_{u,v}}^0 \mathbb{P}(Y_{u,v} = z \mid \mathcal{P}_{u,v}) & \text{if } x = 0. \end{cases} \quad (17)$$

Formulas (16)–(17) are proven in Appendix A.5, and they would be useful for likelihood inference (among others). In analogy to the Tobit INAR time-series model of Weiß et al. (2026), the Tobit CINAR(p_1, p_2) model (15) does not behave *exactly* like a linear model (due to the censoring at zero), but it is reasonable to assume that, despite the presence of some negative AR terms, its dependence structure is often at least *approximately* linear. This conjecture as well as further stochastic properties of the Tobit CINAR(p_1, p_2) model (15) should be analyzed in future research.

3. Parameter Estimation

In this section, we deal with methods for parameter estimation, where all estimators are based on the rectangular segment $X_{1,1}, \dots, X_{n_1, n_2}$ from $(X_{s,t})$ with $n_1, n_2 \in \mathbb{N}$. For the stationary CINAR random field model, parameter estimation can be done by inserting the empirical instead of the theoretical autocorrelations into the respective YW equations

(recall Proposition 2.1.3) and solving them, which leads to the YW estimates. Moreover, the conditional expectation and distribution according to Proposition 2.1.4 can be used to compute the CLS and CML estimates. All three estimation approaches have also been considered for the classical INAR(1, 1) random field model, see Ghodsi et al. (2012), Ghodsi (2015), and Sassi and Parařba (2023). For the sake of uniqueness and comparability to existing INAR results, we consider the reparametrization $\theta_{ij} = \alpha \cdot \phi_{ij}$, i.e., we estimate the parameters $\boldsymbol{\theta} = (\theta_{01}, \dots, \theta_{p_1, p_2})^\top$ (note the lexicographic ordering of the parameters θ_{ij} within $\boldsymbol{\theta}$), where $\sum_{(i,j) \in \mathcal{S}} \theta_{ij} = \alpha$ and $\phi_{ij} = \theta_{ij}/\alpha$. In addition, we estimate the relevant parameters of the innovations process, such as their mean μ_ε and possibly the variance σ_ε^2 . Note that if the innovations follow a Poi-distribution, then the innovations are already fully characterized by solely μ_ε .

3.1. Yule–Walker Estimation

It is well-known that YW estimators are based on the ACF of the respective model. We have shown that for $p_1 = p_2 = 1$, the ACF of the CINAR random field coincides with the ACF of the ordinary INAR(1, 1) random field if the coefficients $\theta_{ij} = \alpha\phi_{ij}$ are replaced by α_{ij} , recall Section 2.2. Consequently, we expect strong similarities to the YW estimator for the INAR(1, 1) random field, which has been derived by Ghodsi et al. (2012). Nevertheless, we present the derivation in order to account for the higher model orders. It should be noted, however, that the YW estimator derived here extends directly to higher-order INAR random fields (3) according to Silbernagel and Weiß (2026a) (if the coefficients are replaced accordingly). From (7), we know that

$$\boldsymbol{\rho} = \mathbf{P} \cdot \boldsymbol{\theta}, \quad (18)$$

where $\boldsymbol{\theta} = (\theta_{ij})_{(i,j) \in \mathcal{S}}$, $\boldsymbol{\rho} = (\rho(k, l))_{(k,l) \in \mathcal{S}}$ and $\mathbf{P} = (\rho(k-i, l-j))_{(k,l),(i,j) \in \mathcal{S}}$. Since $\rho(k, l) = \rho(-k, -l)$ for all $k, l \in \mathbb{Z}$, we replace $\rho(k-i, l-j)$ with $\rho(-k+i, -l+j)$ if $k-i < 0$, and $\rho(0, l-j)$ with $\rho(0, -l+j)$ if $k-i = 0$ and $l-j < 0$. This way, only autocorrelations $\rho(k, l)$ with $(k, l) \in \mathcal{S}$ or $k \in \{1, \dots, p_1\}$ and $l \in \{-1, \dots, -p_2\}$ appear in (18). In case of a first-order model ($p_1 = p_2 = 1$), this yields $\boldsymbol{\rho} = (\rho(0, 1), \rho(1, 0), \rho(1, 1))^\top$ and

$$\mathbf{P} = \begin{pmatrix} 1 & \rho(-1, 1) & \rho(-1, 0) \\ \rho(1, -1) & 1 & \rho(0, -1) \\ \rho(1, 0) & \rho(0, 1) & 1 \end{pmatrix} = \begin{pmatrix} 1 & \rho(1, -1) & \rho(1, 0) \\ \rho(1, -1) & 1 & \rho(0, 1) \\ \rho(1, 0) & \rho(0, 1) & 1 \end{pmatrix}.$$

Note that the difference to Ghodsi et al. (2012) comes from a different ordering of the coefficients (we uniquely use a lexicographic ordering). After replacing all autocorrelations $\rho(k, l)$ in $\boldsymbol{\rho}$ and \mathbf{P} from (18) by their sample analogs $\hat{\rho}(k, l) := \hat{\gamma}(k, l)/\hat{\gamma}(0, 0)$, we denote this vector and matrix by $\hat{\boldsymbol{\rho}}$ and $\hat{\mathbf{P}}$, respectively, where the sample ACvF $\hat{\gamma}(k, l)$ is defined by

$$\hat{\gamma}(k, l) := \frac{1}{n_1 n_2} \sum_{s=1+k}^{n_1} \sum_{t=1+l}^{n_2-l} (X_{s,t} - \bar{X})(X_{s-k,t-l} - \bar{X}) \quad \text{with} \quad \bar{X} = \frac{1}{n_1 n_2} \sum_{s=1}^{n_1} \sum_{t=1}^{n_2} X_{s,t}.$$

Now, the YW estimator $\hat{\boldsymbol{\theta}}_{\text{YW}} = (\hat{\theta}_{\text{YW};ij})_{(i,j) \in \mathcal{S}}$ of $\boldsymbol{\theta}$ is obtained by solving

$$\hat{\boldsymbol{\theta}}_{\text{YW}} = \hat{\mathbf{P}}^{-1} \hat{\boldsymbol{\rho}}. \quad (19)$$

Therefore, $\hat{\alpha}_{\text{YW}} = \sum_{(i,j) \in \mathcal{S}} \hat{\theta}_{\text{YW};ij}$ and $\hat{\phi}_{\text{YW};ij} = \hat{\theta}_{\text{YW};ij}/\hat{\alpha}_{\text{YW}}$. Moreover, using (6), μ_ε and σ_ε^2 are estimated by

$$\hat{\mu}_{\text{YW};\varepsilon} = \bar{X} \cdot (1 - \hat{\alpha}_{\text{YW}}) \quad \text{and} \quad \hat{\sigma}_{\text{YW};\varepsilon}^2 = \hat{\sigma}_X^2 \cdot (1 - \hat{\alpha}_{\text{YW}}) - \hat{\alpha}_{\text{YW}} \cdot \hat{\mu}_{\text{YW};\varepsilon}, \quad (20)$$

where $\hat{\sigma}_X^2 := \hat{\gamma}(0, 0)$. Note that while the definition of the YW estimator is intuitive, it may lead to inadmissible estimates in practice, i.e., estimates that violate the parameter constraints according to Definition 2.0.1.

3.2. Conditional Least Squares Estimation

The CLS estimator of $\boldsymbol{\theta} = (\theta_{01}, \dots, \theta_{p_1, p_2}, \mu_\varepsilon)^\top$, the parameters being involved in the conditional mean (10), is given by the statistic $\hat{\boldsymbol{\theta}}_{\text{CLS}} := \arg \min_{\boldsymbol{\theta}} Q_{n_1, n_2}(\boldsymbol{\theta})$ minimizing the sum of squared deviations

$$Q_{n_1, n_2}(\boldsymbol{\theta}) := \sum_{s=p_1+1}^{n_1} \sum_{t=p_2+1}^{n_2} (X_{s,t} - \mathbb{E}(X_{s,t} | \mathcal{P}_{s,t}))^2 = \sum_{s=p_1+1}^{n_1} \sum_{t=p_2+1}^{n_2} \left(X_{s,t} - \mu_\varepsilon - \sum_{(i,j) \in \mathcal{S}} \theta_{ij} X_{s-i,t-j} \right)^2.$$

Besides a direct numerical (constrained) minimization of $Q_{n_1, n_2}(\boldsymbol{\theta})$, also closed-form expressions for the CLS estimator can be derived. The partial derivatives of $Q_{n_1, n_2}(\boldsymbol{\theta})$ are given by

$$\frac{\partial}{\partial \mu_\varepsilon} Q_{n_1, n_2}(\boldsymbol{\theta}) = -2 \sum_{s=p_1+1}^{n_1} \sum_{t=p_2+1}^{n_2} \left(X_{s,t} - \mu_\varepsilon - \sum_{(i,j) \in \mathcal{S}} \theta_{ij} X_{s-i, t-j} \right), \quad (21)$$

$$\frac{\partial}{\partial \theta_{k,l}} Q_{n_1, n_2}(\boldsymbol{\theta}) = -2 \sum_{s=p_1+1}^{n_1} \sum_{t=p_2+1}^{n_2} \left(X_{s-k, t-l} \cdot \left(X_{s,t} - \mu_\varepsilon - \sum_{(i,j) \in \mathcal{S}} \theta_{ij} X_{s-i, t-j} \right) \right) \quad \text{for } (k, l) \in \mathcal{S}. \quad (22)$$

For notational convenience, we write $n := (n_1 - p_1)(n_2 - p_2)$. Equating (21) to zero, we obtain

$$\mu_\varepsilon = \frac{1}{n} \sum_{s=p_1+1}^{n_1} \sum_{t=p_2+1}^{n_2} \left(X_{s,t} - \sum_{(i,j) \in \mathcal{S}} \theta_{ij} X_{s-i, t-j} \right). \quad (23)$$

Then, equating (22) to zero and substituting μ_ε , we get

$$\sum_{(i,j) \in \mathcal{S}} \theta_{ij} \tilde{\gamma}((i, j), (k, l)) = \tilde{\gamma}((k, l), (0, 0)), \quad (k, l) \in \mathcal{S}, \quad (24)$$

where

$$\tilde{\gamma}((i, j), (k, l)) := \left(\frac{1}{n} \sum_{s=p_1+1}^{n_1} \sum_{t=p_2+1}^{n_2} X_{s-i, t-j} \cdot X_{s-k, t-l} \right) - \left(\frac{1}{n} \sum_{s=p_1+1}^{n_1} \sum_{t=p_2+1}^{n_2} X_{s-i, t-j} \right) \cdot \left(\frac{1}{n} \sum_{s=p_1+1}^{n_1} \sum_{t=p_2+1}^{n_2} X_{s-k, t-l} \right).$$

Combining (23) and (24) is equivalent to solving

$$\mathbf{A} \cdot \boldsymbol{\theta} = \mathbf{b}, \quad (25)$$

where \mathbf{b} is the $(|\mathcal{S}| + 1) = (p_1 + 1)(p_2 + 1)$ -dimensional vector defined by

$$\mathbf{b} = \sum_{s=p_1+1}^{n_1} \sum_{t=p_2+1}^{n_2} ((X_{s,t} \cdot X_{s-i, t-k})_{(i,j) \in \mathcal{S}}, X_{s,t})^\top,$$

and \mathbf{A} is the symmetric $((p_1 + 1)(p_2 + 1)) \times ((p_1 + 1)(p_2 + 1))$ -dimensional matrix

$$\mathbf{A} = \sum_{s=p_1+1}^{n_1} \sum_{t=p_2+1}^{n_2} \begin{pmatrix} (X_{s-i, t-j} \cdot X_{s-k, t-l})_{(i,j), (k,l) \in \mathcal{S}} & (X_{s-i, t-j})_{(i,j) \in \mathcal{S}} \\ (X_{s-k, t-l})_{(k,l) \in \mathcal{S}} & 1 \end{pmatrix},$$

which contains the matrix $(X_{s-i, t-j} \cdot X_{s-k, t-l})_{(i,j), (k,l) \in \mathcal{S}}$ in the upper left corner. Hence, the CLS estimator $\hat{\boldsymbol{\theta}}_{\text{CLS}} = \hat{\boldsymbol{\theta}}_{\text{CLS}}(n)$ of $\boldsymbol{\theta}$ is computed from

$$\hat{\boldsymbol{\theta}}_{\text{CLS}} = \mathbf{A}^{-1} \mathbf{b}.$$

Note that these statistics truly minimize $Q_{n_1, n_2}(\boldsymbol{\theta})$, since all second derivatives are positive except for trivial cases (recall that both $(X_{s,t})$ and $(\varepsilon_{s,t})$ are non-negative counts):

$$\begin{aligned} \frac{\partial^2}{\partial \theta_{kl} \partial \mu_\varepsilon} Q_{n_1, n_2}(\boldsymbol{\theta}) &= +2 \sum_{s=p_1+1}^{n_1} \sum_{t=p_2+1}^{n_2} X_{s-k, t-l} > 0, \\ \frac{\partial^2}{\partial \theta_{ij} \partial \theta_{kl}} Q_{n_1, n_2}(\boldsymbol{\theta}) &= +2 \sum_{s=p_1+1}^{n_1} \sum_{t=p_2+1}^{n_2} X_{s-k, t-l} X_{s-i, t-j} > 0, \\ \frac{\partial^2}{\partial \mu_\varepsilon^2} Q_{n_1, n_2}(\boldsymbol{\theta}) &= +2n > 0. \end{aligned}$$

Compare these estimators with those of Sassi and Paraíba (2023), who have proposed a CLS estimation procedure for INAR(1, 1) random field models: $\hat{\boldsymbol{\theta}}_{\text{CLS}}$ matches their estimator if $p_1 = p_2 = 1$ and if θ_{ij} is substituted by α_{ij} . Let us stress that the conditional expectations of the CINAR(p_1, p_2) and INAR(p_1, p_2) models coincide in general if $\theta_{ij} = \alpha \phi_{ij}$ is replaced by α_{ij} , see Silbernagel and Weiß (2026a). Therefore, $\hat{\boldsymbol{\theta}}_{\text{CLS}}$ transfers directly to INAR(p_1, p_2) models with appropriately adjusted coefficients. Finally, $\hat{\alpha}_{\text{CLS}} = \sum_{(i,j) \in \mathcal{S}} \hat{\theta}_{\text{CLS}; ij}$ and $\hat{\phi}_{\text{CLS}; ij} = \hat{\theta}_{\text{CLS}; ij} / \hat{\alpha}_{\text{CLS}}$ as before.

3.3. Conditional Maximum Likelihood Estimation

In order to apply the CML procedure, the CINAR model has to be fully specified, i.e., we also need to specify the innovations' distribution. For example, in the case of a Poi-CINAR model with $\varepsilon_{s,t} \sim \text{Poi}(\mu_\varepsilon)$, the full model parametrization is given by $\boldsymbol{\vartheta} = (\theta_{01}, \dots, \theta_{p_1, p_2}, \mu_\varepsilon)^\top$, whereas the NB-CINAR model requires an additional dispersion parameter, e.g., $\boldsymbol{\vartheta} = (\theta_{01}, \dots, \theta_{p_1, p_2}, \mu_\varepsilon, I_\varepsilon)^\top$ with $I_\varepsilon = \sigma_\varepsilon^2 / \mu_\varepsilon > 1$, recall Example 2.2.1. In order to express the conditional likelihood function of the CINAR(p_1, p_2) random field, we have to split the available rectangular data segment $\mathcal{X}_{1,1}^{n_1, n_2} := \{X_{1,1}, \dots, X_{n_1, n_2}\}$ into two parts, namely into ‘‘upper-right rectangle’’ $\mathcal{X}_{p_1+1, p_2+1}^{n_1, n_2} := \{X_{p_1+1, p_2+1}, \dots, X_{n_1, n_2}\}$ and the remaining ‘‘bottom-left boundary’’ $\mathcal{X}_{1,1}^{n_1, n_2} \setminus \mathcal{X}_{p_1+1, p_2+1}^{n_1, n_2}$. Then, the conditional likelihood function is given by

$$L(\boldsymbol{\vartheta} \mid \mathcal{X}_{1,1}^{n_1, n_2} \setminus \mathcal{X}_{p_1+1, p_2+1}^{n_1, n_2}) := \mathbb{P}(\mathcal{X}_{p_1+1, p_2+1}^{n_1, n_2} \mid \mathcal{X}_{1,1}^{n_1, n_2} \setminus \mathcal{X}_{p_1+1, p_2+1}^{n_1, n_2}) = \prod_{s=p_1+1}^{n_1} \prod_{t=p_2+1}^{n_2} \mathbb{P}(X_{s,t} \mid \mathcal{P}_{s,t}),$$

where the conditional probabilities are computed according to Proposition 2.1.4. Here, the factorization of the likelihood function follows from the unilateral model recursion (4) and the expression (9) for the conditional probabilities. Then, the log-likelihood function is given by

$$\ell(\boldsymbol{\vartheta}) = \log L(\boldsymbol{\vartheta}) = \sum_{s=p_1+1}^{n_1} \sum_{t=p_2+1}^{n_2} \log \mathbb{P}(X_{s,t} \mid \mathcal{P}_{s,t}).$$

The maximum likelihood estimator is defined as the parameter which maximizes $\ell(\boldsymbol{\vartheta})$ (and thus $L(\boldsymbol{\vartheta})$) and, hence, makes the observed data most ‘‘plausible’’. Recall that the conditional distributions according to Proposition 2.1.4 are much simpler than those of the classical INAR random fields in Ghodsi (2015); Silbernagel and Weiß (2026a), as they involve only one convolution. In practice, the CML estimates $\hat{\boldsymbol{\vartheta}}_{\text{CML}}$ are determined by a constrained numerical optimization of the log-likelihood function ℓ (with $\hat{\alpha}_{\text{CML}} = \sum_{(i,j) \in \mathcal{S}} \hat{\theta}_{\text{CML};ij}$ and $\hat{\phi}_{\text{CML};ij} = \hat{\theta}_{\text{CML};ij} / \hat{\alpha}_{\text{CML}}$), where the above YW or CLS estimates can be used as initial values for the numerical routine. Note that it is also possible to numerically approximate the standard errors of the CML estimates (namely from the negative Hessian of ℓ at the maximum, i.e., the observed Fisher information) as well as to compute information criteria for model selection, see Weiß (2018, Remark B.2.1.2) for details. These computations are later illustrated in Section 5.

4. Performance of Parameter Estimation

In order to investigate the finite-sample performance of the estimation approaches derived in Section 3, we did a comprehensive simulation study with data generating processes (DGPs) from various types of CINAR models. More precisely, in analogy to Ghodsi et al. (2012); Ghodsi (2015), we considered Poi-CINAR(1, 1) random fields with $\mu_\varepsilon = 1$ and AR parameters $(\theta_{01}, \theta_{10}, \theta_{11})$ equal to (0.1, 0.1, 0.1), (0.2, 0.2, 0.5), or (0.3, 0.4, 0.1) on the one hand (recall that $\theta_{ij} = \alpha \phi_{ij}$), and corresponding NB-counterparts (i.e., with an NB-marginal distribution for $X_{s,t}$) on the other hand. Here, the required innovations' distribution is computed according to Example 2.2.1 with $\mu_\varepsilon = 1$ and $I_\varepsilon := \sigma_\varepsilon^2 / \mu_\varepsilon = 2$ throughout. Finally, we also considered the Poi-CINAR(2, 2) model with $\mu_\varepsilon = 1$ and $(\theta_{01}, \theta_{02}, \theta_{10}, \theta_{11}, \theta_{12}, \theta_{20}, \theta_{21}, \theta_{22})$ equal to (0.1, ..., 0.1) or (0.15, 0.1, 0.15, 0.15, 0.05, 0.1, 0.05, 0.1). For each DGP, the sample sizes (n_1, n_2) are chosen as (10, 10), (15, 15), (20, 20), and (50, 50), respectively. In order to ensure stationarity, we used a burn-in period of ‘‘width’’ 100, i.e., we simulated $(n_1 + 100) \times (n_2 + 100)$ counts in order to use the $n_1 \times n_2$ ‘‘most recent’’ counts for parameter estimation. Although our CINAR approach avoids multiple convolutions, the computing time for the constrained optimization via R's `constrOptim` still quickly increases with increasing model complexity (especially for CML estimation). Therefore, we had to restrict the number of replication to 1,000 per scenario. The full tables with means and standard deviations of the obtained estimates are summarized in Appendix B, which are complemented by illustrative boxplots in the subsequent discussion.

Let us start our analyses with the Poi-CINAR(1, 1) random field. As can be seen from Table B.1 in the appendix, in the setting $(\theta_{01}, \theta_{10}, \theta_{11}) = (0.1, 0.1, 0.1)$ with low AR parameters, all three estimation methods work similarly well. This clearly changes, however, in the remaining two scenarios, where at least one of the parameters is rather large. Then, CLS and in particular YW estimation lead to a strong negative bias for the large dependence parameters, which, in turn, causes a strong positive bias for μ_ε . The CML estimator, by contrast, shows only negligible bias throughout,

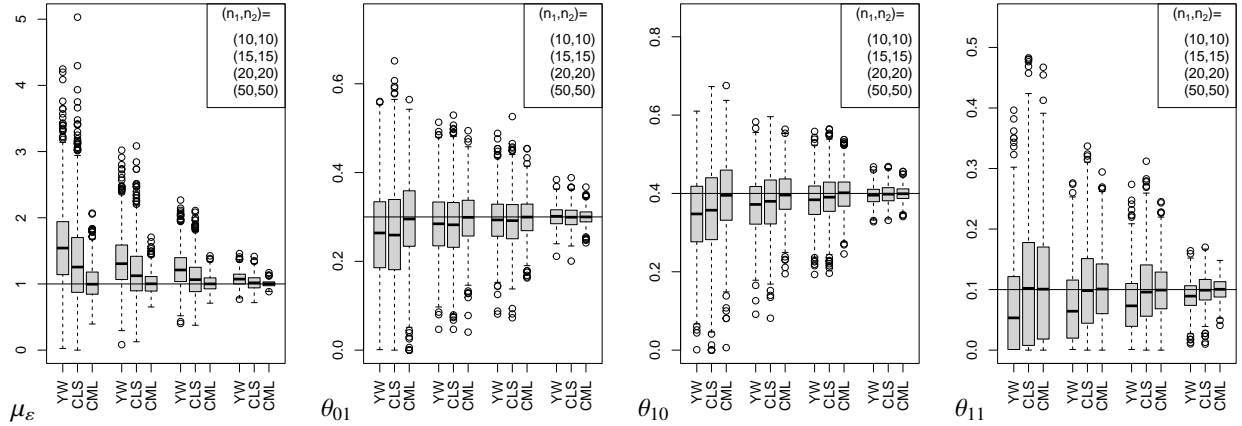


Fig. 2: Boxplots of simulated estimates for Poi-CINAR(1, 1) random field (true parameter values at horizontal lines), with increasing sample size (n_1, n_2) from left to right.

and also its standard deviations are substantially lower than those of YW and CLS. This discrepancy in performance can also be seen in Figure 2, where the boxplots for the scenario $(\theta_{01}, \theta_{10}, \theta_{11}) = (0.3, 0.4, 0.1)$ are shown. Altogether, we conclude that the Poi-CINAR(1, 1)'s parameters should be estimated with the CML approach, whereas YW and CLS are only recommended for initializing the required numerical optimization routine.

Next, we consider the NB-CINAR(1, 1) DGPs, the innovations of which uniquely have the dispersion ratio $I_\varepsilon = 2$, i.e., they exhibit a substantial extent of overdispersion. Recall that CLS is only able to estimate the parameters being involved in the conditional mean, i.e., it cannot estimate the value of I_ε . The latter is only achieved by YW and CML (more precisely, by “N-CML”, see the discussion below). The results in Table B.2 and Figure 3 confirm our previous conclusion that YW and CLS are only competitive to CML if the AR parameters are low. Otherwise, we have the same problems with bias and standard deviation described before, with the YW estimator of I_ε exhibiting a strong negative bias. So our previous recommendation of using CML for parameter estimation extends to the NB-case as well. However, there is one point to be noted. The outstanding performance of CML estimation clearly depends on choosing the adequate model type. To analyze the effect of a possible model misspecification, we did not only use the NB-CINAR(1, 1) likelihood function for parameter estimation (labeled as “N-CML”), but also falsely the one of a Poi-CINAR(1, 1) random field (labeled as “P-CML”). In Figure 3, the misspecified case is further highlighted by white boxes. It gets clear that under model misspecification, the CML estimates are affected by a strong bias that also does not vanish with increasing sample size. Then, for large sample sizes, even YW and CLS show a better performance than CML. So while CML is generally recommended due to its outstanding performance, it should always be accompanied by subsequent checks of model adequacy. A substantial discrepancy between CLS and CML, in turn, should be interpreted as a warning sign of a possible model misspecification.

Finally, we turn to the higher-order case, namely the aforementioned Poi-CINAR(2, 2) DGPs, see Table B.3 and Figure 4 for a summary. Here, we did not use YW anymore as it becomes more and more difficult to obtain admissible estimates (i.e., satisfying all parameter constraints) with increasing number of parameters. On the other hand, we extended our analyses of a possible model misspecification by considering both the CLS and CML estimates corresponding to falsely fitting a Poi-CINAR(1, 1) model (labeled as “CLS-1” and “CML-1”, respectively, and again highlighted by white boxes in Figure 4). The results obtained are consistent with our previous observations. For a correct model specification, CLS improves with increasing sample size, but is clearly outperformed by CML in terms of both bias and standard deviation. So using CLS for initial and CML for final parameter estimation is still recommended. If the model order is misspecified, by contrast, both estimation approaches show a poor performance and a non-vanishing bias also for large sample sizes. So again, we advise to not do model fitting without a subsequent model diagnosis.

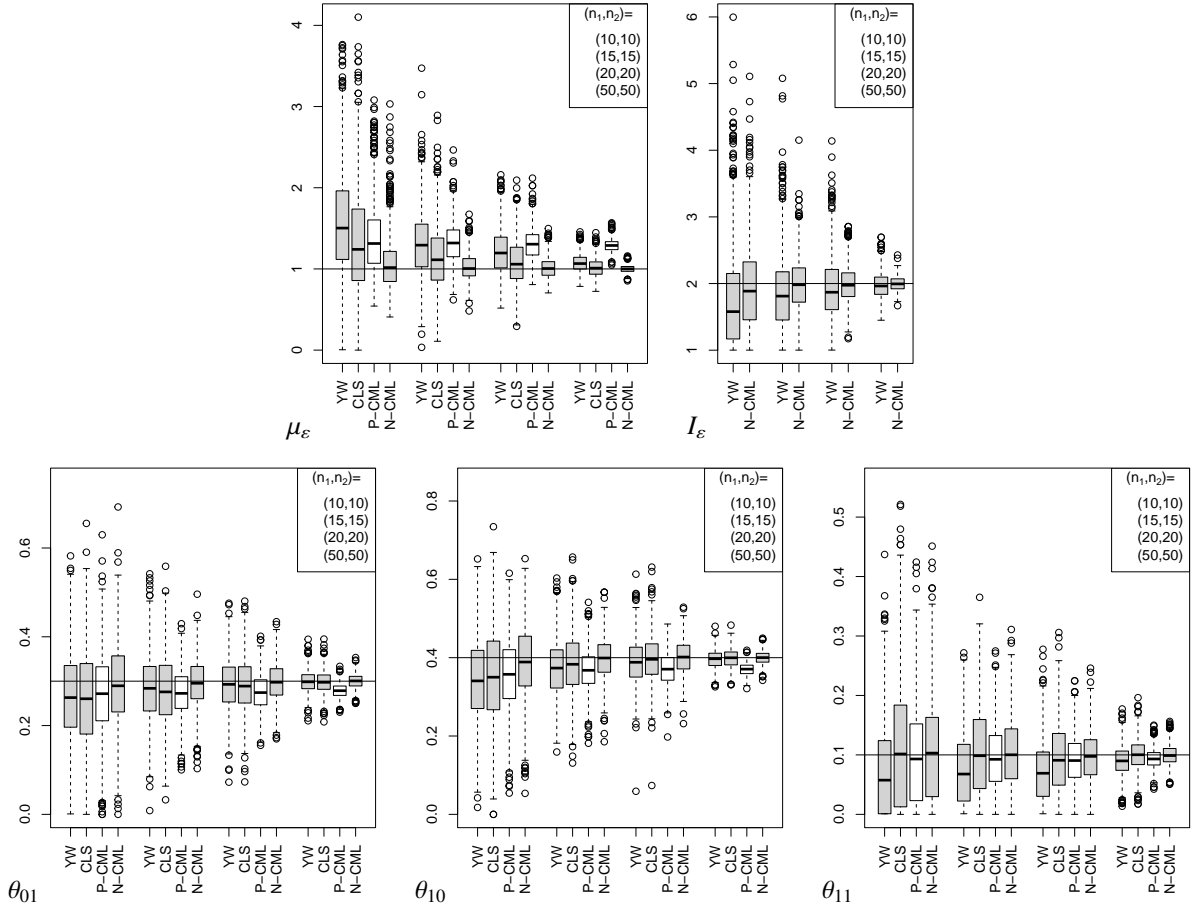


Fig. 3: Boxplots of simulated estimates for NB-CINAR(1, 1) random field (true parameter values at horizontal lines), with increasing sample size (n_1, n_2) from left to right. Boxplots with white background correspond to model misspecification.

5. Data Example: Yields from an Agricultural Experiment

We consider the data set published in the Appendix of Iyer (1942), which is also offered by the R package “agridat” through the command `iyer.wheat.uniformity`. The data are plotted in Figure 5 (a), in the same arrangement as in the table in Iyer (1942). They describe the result of an agricultural experiment about harvesting wheat in an experimental field that was divided into $n_1 \times n_2 = 25 \times 80$ plots of size 5 ft \times 5 ft, with the grain yield $X_{s,t}$ reported in units of half an ounce. The resulting sample PMF in Figure 5 (b) is quite similar to a Poi-distribution with parameter equal to the sample mean $\hat{\mu}_X = 33.8425$. The close agreement to a Poi-distribution is also confirmed by the sample dispersion ratio $\hat{\sigma}_X^2 / \hat{\mu}_X \approx 1.129$, which shows that the data are nearly equidispersed. Finally, the sample ACF in part (c) shows substantially positive ACF values that quickly decay with increasing absolute spatial lag such that altogether, it appears reasonable to try to model the data by an AR-type model having a Poi-marginal distribution, as it is the case for the Poi-CINAR model.

We start our analyses with the (full) Poi-CINAR(1, 1) model according to Section 2.2. The corresponding CML estimates are determined by a numerical optimization of the log-likelihood function ℓ , where the YW or CLS estimates can be used as initial values for the numerical routine. Here, in view of a unique parametrization across the different estimation approaches, we use the parametrization with $\theta_{ij} = \alpha \phi_{ij}$. Approximate standard errors for the CML estimates are computed from the negative Hessian of ℓ at the maximum (observed Fisher information), see Remark B.2.1.2 in Weiß (2018) for details. The results are summarized in the first line of Table 1. If judging the estimates on a 5 %-level, it gets clear that the estimate θ_{11} (expressing a diagonal dependence) is not significantly different from zero, which implies that a simplified CINAR(1, 1) model with $\theta_{11} \equiv 0$ (so with spatial dependence only in

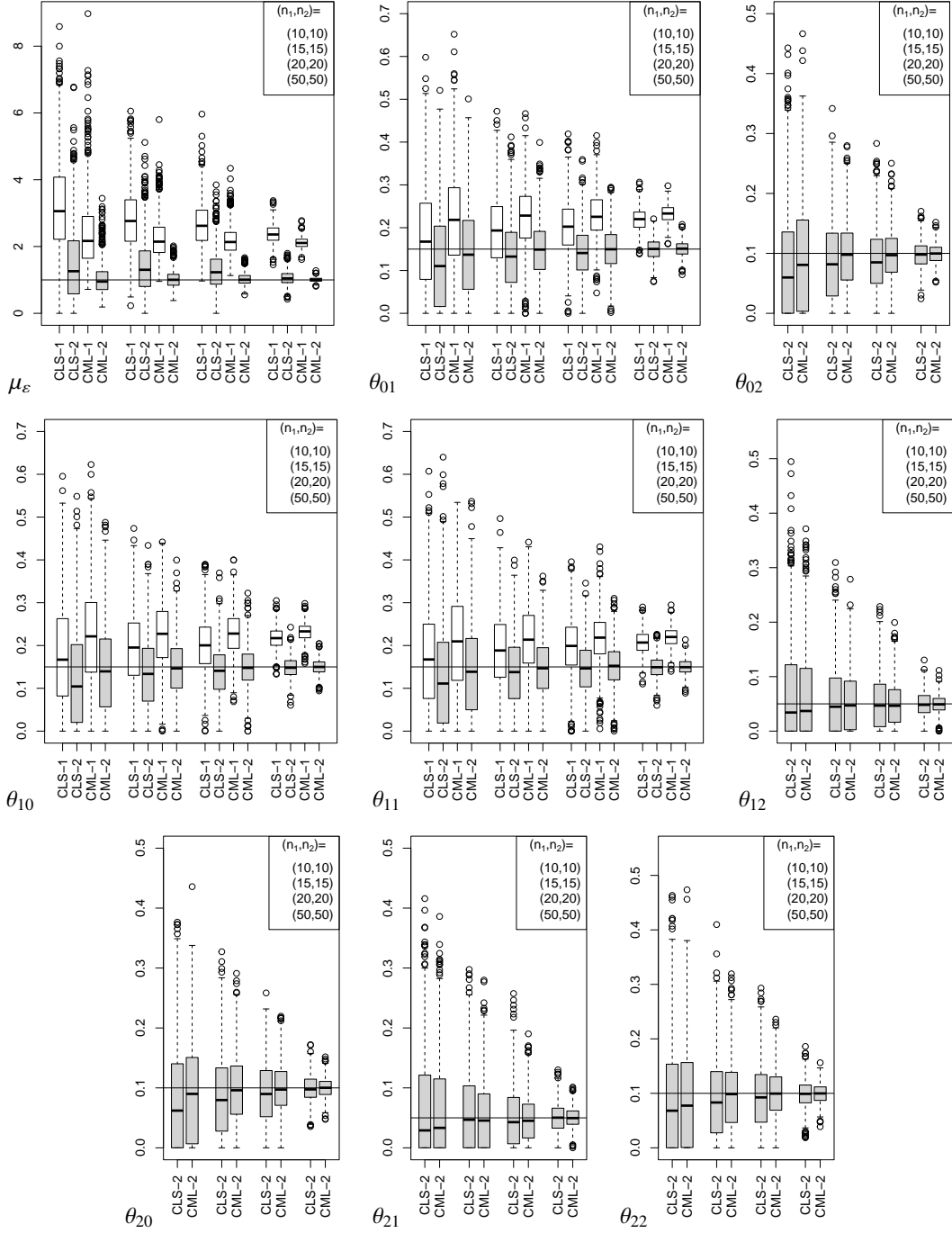


Fig. 4: Boxplots of simulated estimates for Poi-CINAR(2, 2) random field (true parameter values at horizontal lines), with increasing sample size (n_1, n_2) from left to right. Boxplots with white background correspond to model misspecification.

horizontal and vertical direction) appears to be another reasonable candidate model; see Table 1 for the corresponding model fit. In order to choose among the different candidate models, a common approach is to use information criteria such as Akaike's or the Bayesian one (AIC or BIC, respectively). Since these criteria are computed from the *conditional* log-likelihood and since we shall later also compare to different model orders, we use a re-scaled maximized log-likelihood ℓ_{\max} like in Weiß (2018, Remark B.2.1.2) for AIC and BIC computation, namely $n_1 n_2 / n_\ell \cdot \ell_{\max}$ where

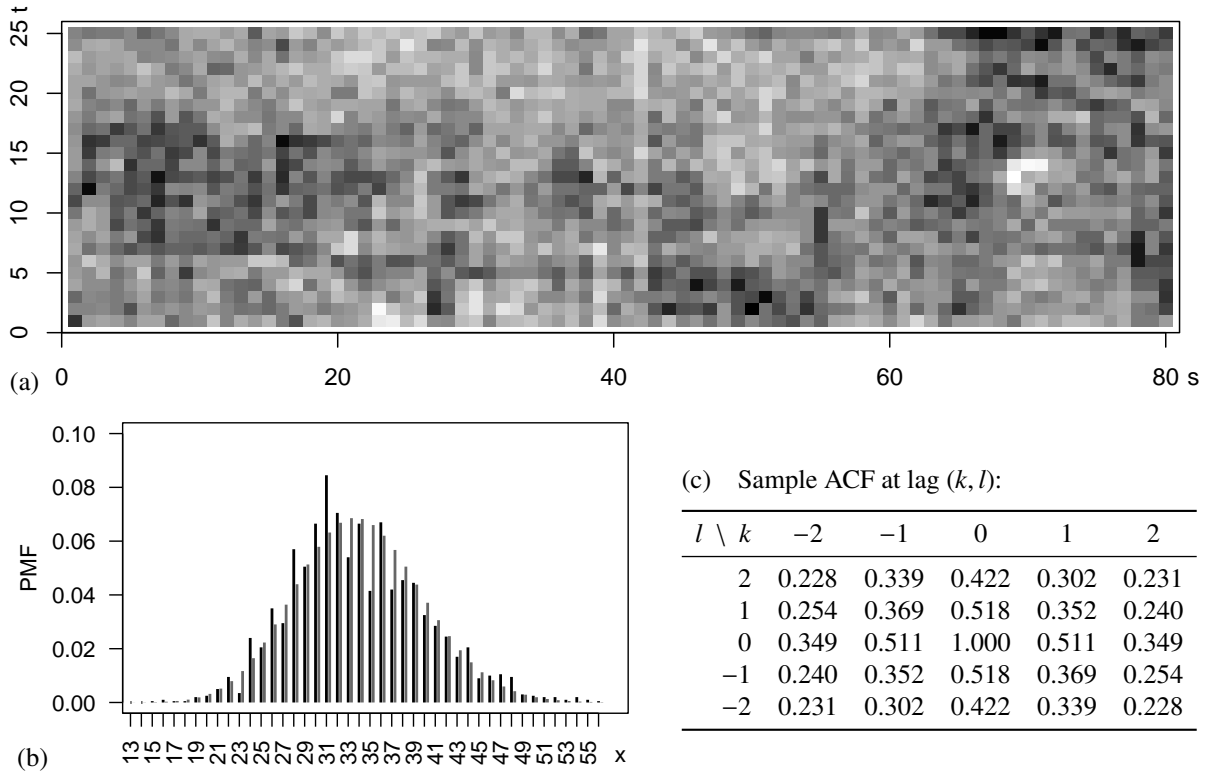


Fig. 5: Wheat yields data from Section 5: (a) gray-scale plot of data, where counts range between 0 (white) and 56 (black), (b) sample PMF (black) compared to Poi(33.8425)-PMF (gray), and (c) sample ACF for spatial lags (k, l) with $-2 \leq k, l \leq 2$.

n_ℓ expresses the number of summands in the conditional log-likelihood function. From the results in Table 1, we recognize that both criteria prefer the simplified CINAR(1, 1) model.

In order to check the adequacy of the selected model, we use the standardized Pearson residuals and the PIT histogram for model diagnostics (computed according to Proposition 2.1.4), which are established tools in the analysis of count time series (Weiß, 2018, Section 2.4) as well as spatial count data (Jung and Glaser, 2022). The mean and variance of the Pearson residuals in Figure 6 are rather close to zero and one, respectively, which is in favor of model validity. Also the PIT histogram is reasonably close to uniformity and thus confirms an adequate model choice. If comparing the sample ACF of the Pearson residuals to those of the original data, recall Figure 5 (c), we recognize a strong reduction of absolute value, i.e., most part of the apparent dependencies are covered by the simplified CINAR(1, 1) model. A closer look, however, still reveals relatively large values at lags $(0, \mp 2)$ and $(\mp 2, 0)$, which indicates that a second-order CINAR model might be better suited for the wheat yields data.

Hence, we first fitted a full CINAR(2, 2) model to the wheat yields data, see the first line in Table 2. We recognize that only the estimates for θ_{02}, θ_{01} (vertical dependence) and θ_{10}, θ_{20} (horizontal dependence) are significantly different from zero. These results nicely agree with our first-order findings, and it extends the dependence structure in those directions where relatively large values of the CINAR(1, 1) residuals' ACF were detected, recall Figure 7 (a). Table 2 also shows the estimates for the simplified CINAR(2, 2) model. From the given AIC and BIC values, we conclude that this model does not only outperform the full CINAR(2, 2) model, but also any of the first-order models from Table 1. Finally, let us look at the correspondings model diagnostics in Figure 7. While PIT histogram and the Pearson residuals' mean and variance indicate a similar performance as for the simplified CINAR(1, 1) model, we recognize a clear improvement in terms of their ACF, where all values deviate from zero only in the second decimal place. Although none of the criteria in Figure 7 indicates a perfect adequacy, it seems that the simplified CINAR(2, 2) model constitutes a reasonable “workhorse model” for the wheat yields data.

Table 1: Wheat yields data from Section 5: CML estimates (standard errors in parentheses) and information criteria for CINAR(1, 1) candidate models.

Model	μ_ε	θ_{01}	θ_{10}	θ_{11}	AIC	BIC
full	11.215 (0.474)	0.287 (0.022)	0.358 (0.022)	0.023 (0.021)	11932.9	11955.3
simplified	11.428 (0.439)	0.296 (0.021)	0.365 (0.021)	0	11932.2	11949.0

(a) **Standardized Pearson residuals:**

mean -0.004 , variance 0.983 ,
and sample ACF at lag (k, l) :

$l \setminus k$	-2	-1	0	1	2
2	0.025	0.067	0.119	0.059	0.058
1	0.025	0.013	0.022	0.074	-0.010
0	0.083	0.007	1.000	0.007	0.083
-1	-0.010	0.074	0.022	0.013	0.025
-2	0.058	0.059	0.119	0.067	0.025

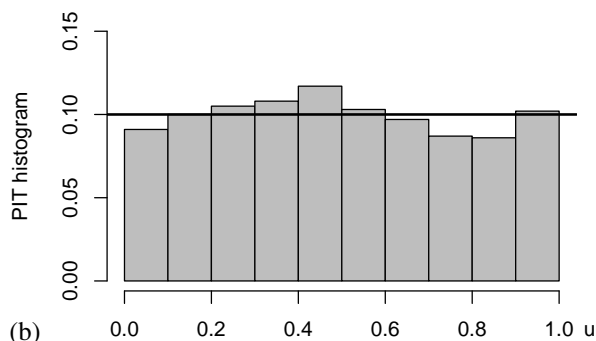


Fig. 6: Simplified CINAR(1, 1) model for wheat yields data according to Table 1: (a) mean, variance, and sample ACF of Pearson residuals; (b) PIT histogram.

6. Conclusions and Future Research

In this article, we proposed the CINAR family for modeling count random fields, which exhibits the same auto-correlation structure as ordinary INAR random fields, but which can be equipped with, e.g., a Poi- or NB-marginal distribution. More generally, having specified the innovations' distribution, the observations' marginal distribution is fully known, which differs from the case of INAR random fields. A further advantage is a simpler computation of conditional probabilities and, thus, likelihood functions. In fact, we developed three approaches for parameter estimation (YW, CLS, and CML) and analyzed their performance by simulations. If the model is correctly specified, the CML approach clearly surpasses its competitors, but it performs poorly under model misspecification. So model fitting should not be done without subsequent checks of model adequacy. This was exemplified by our data example on wheat yields from an agricultural experiment, which also demonstrated the practical relevance of our novel CINAR family.

There are various directions for future research. First, one may adapt the CINAR model to different INAR-like models for counts, e.g., to the iterated-thinning INAR model having both NB-distributed observations and innovations, see Aleksandrov et al. (2024) for a comprehensive discussion. Second, one could develop a CINAR-like model for bounded counts (i.e., where the range is bounded from above by some integer value $N \in \mathbb{N}$), where the binomial AR model of Weiß (2009) appears to be a possible starting point. Finally, as already discussed in some detail in Section 2.3, a multilateral extension of the CINAR model as well as a Tobit approach for negative dependencies appear to be appealing challenges for future research.

References

- Boris Aleksandrov, Christian H Weiß, Simon Nik, Maxime Faymonville, and Carsten Jentsch. Modelling and diagnostic tests for Poisson and negative-binomial count time series. *Metrika*, 87(7):843–887, 2024. doi: 10.1007/s00184-023-00934-0.
- Abdulhamid A. Alzaid and Mohamed A. Al-Osh. An integer-valued pth-order autoregressive structure (INAR(p)) process. *Journal of Applied Probability*, 27(2):314–324, 1990. doi: 10.2307/3214650.
- Sabyasachi Basu and Gregory C Reinsel. Properties of the spatial unilateral first-order ARMA model. *Advances in Applied Probability*, 25(3): 631–648, 1993. doi: 10.2307/1427527.

Table 2: Wheat yields data from Section 5: CML estimates (standard errors in parentheses) and information criteria for CINAR(2,2) candidate models.

Model	μ_ε	θ_{02}	θ_{01}	θ_{10}	θ_{11}	θ_{12}	θ_{20}	θ_{21}	θ_{22}	AIC	BIC
full	9.420 (0.542)	0.233 (0.025)	0.100 (0.023)	0.313 (0.026)	0.002 (0.024)	0.016 (0.020)	0.057 (0.023)	0.000 (0.015)	0.000 (0.021)	11868.0	11918.4
simplified	9.498 (0.481)	0.238 (0.023)	0.104 (0.022)	0.313 (0.025)	0	0	0.065 (0.023)	0	0	11860.2	11888.2

(a) **Standardized Pearson residuals:**

mean -0.004 , variance 0.935 ,
and sample ACF at lag (k, l) :

$l \setminus k$	-2	-1	0	1	2
2	-0.002	0.054	0.032	0.048	0.040
1	0.025	0.018	0.067	0.074	-0.006
0	0.032	0.030	1.000	0.030	0.032
-1	-0.006	0.074	0.067	0.018	0.025
-2	0.040	0.048	0.032	0.054	-0.002

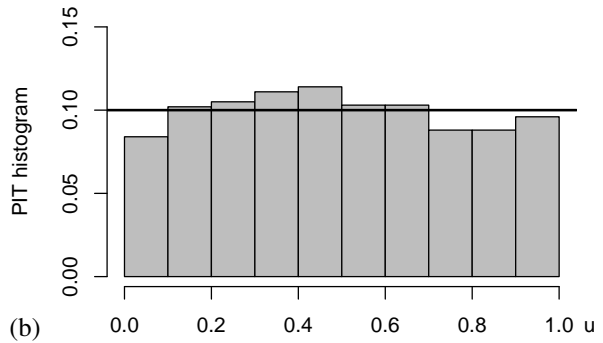


Fig. 7: Simplified CINAR(2,2) model for wheat yields data according to Table 2: (a) mean, variance, and sample ACF of Pearson residuals; (b) PIT histogram.

Julian Besag. Spatial interaction and the statistical analysis of lattice systems. *Journal of the Royal Statistical Society: Series B (Methodological)*, 36(2):192–225, 1974. doi: 10.1111/j.2517-6161.1974.tb00999.x.

Patrick Billingsley. *Probability and Measure*. John Wiley & Sons, Ltd, 3rd ed edition, 1995. ISBN 0471007102.

Azmi Chutoo, Dimitris Karlis, Naushad Mamode Khan, and Vandna Jowaheer. The unilateral spatial autoregressive process for the regular lattice two-dimensional spatial discrete data. *SORT-Statistics and Operations Research Transactions*, 45(1):67–90, 2021. doi: 10.2436/20.8080.02.110.

Jin-Guan Du and Yuan Li. The integer-valued autoregressive (INAR(p)) model. *Journal of Time Series Analysis*, 12(2):129–142, 1991. doi: 10.1111/j.1467-9892.1991.tb00073.x.

Alireza Ghodsi. Conditional maximum likelihood estimation of the first-order spatial integer-valued autoregressive (SINAR(1, 1)) model. *Journal of the Iranian Statistical Society*, 14(2):15–36, 2015. doi: 10.7508/jirss.2015.02.002.

Alireza Ghodsi and Hassan S. Bakouch. Spatial INAR(1,1) model based on mixing Pogram and binomial thinning operators with fitting striga counts. *Communications in Statistics - Theory and Methods*, 54(21):6988–6996, 2025. doi: 10.1080/03610926.2025.2465647.

Alireza Ghodsi, Mahendran Shitan, and Hassan S Bakouch. A first-order spatial integer-valued autoregressive SINAR(1, 1) model. *Communications in Statistics-Theory and Methods*, 41(15):2773–2787, 2012. doi: 10.1080/03610926.2011.560739.

Alireza Ghodsi, Hassan S. Bakouch, and Mahendran Shitan. First-order spatial dependent count integer-valued autoregressive (Sp-DCINAR(1,1)) process. *Communications in Statistics - Simulation and Computation*, 53(12):6050–6060, 2024. doi: 10.1080/03610918.2023.2234681.

Stephanie Glaser. A review of spatial econometric models for count data. Hohenheim Discussion Papers in Business, Economics and Social Sciences 19-2017, Universität Hohenheim, Fakultät Wirtschafts- und Sozialwissenschaften, Stuttgart, 2017. URL <https://hdl.handle.net/10419/168040>.

Robert P. Haining. The moving average model for spatial interaction. *Transactions of the Institute of British Geographers*, 3(2):202–225, 1978. doi: 10.2307/622202.

P. V. Krishna Iyer. Studies with wheat uniformity trial data. I. Size and shape of experimental plots and the relative efficiency of different layouts. *The Indian Journal of Agricultural Science*, 12(1):240–262, 1942. URL https://archive.org/stream/in.ernet.dli.2015.7638/2015_7638_The-Indian-Journal-Of-Agricultural-Science-Vol-xii-1942#page/n267/mode/2up.

Robert C. Jung and Stephanie Glaser. Modelling and diagnostics of spatially autocorrelated counts. *Econometrics*, 10(3), 2022. doi: 10.3390/econometrics10030031.

Dimitris Karlis, Azmi Chutoo, Naushad Mamode Khan, and Vandna Jowaheer. The multilateral spatial integer-valued process of order 1. *Statistica Neerlandica*, 78(1):4–24, 2024. doi: 10.1111/stan.12298.

Gilberto Pereira Sassi and Carolina Costa Mota Paraiba. Conditional least squares estimation for the SINAR(1, 1) process. *Communications in Statistics - Simulation and Computation*, 52(3):945–960, 2023. doi: 10.1080/03610918.2020.1871489.

Angelika Silbernagel and Christian H Weiß. The autocorrelation structure of integer-valued autoregressive random fields. *Statistics & Probability Letters*, 233:110681, 2026a. doi: 10.1016/j.spl.2026.110681.

Angelika Silbernagel and Christian H Weiß. The integer-valued moving-average random field. *Preprint*, 2026b. URL <https://arxiv.org/abs/2604.13779>.

Atefeh Tabandeh and Alireza Ghodsi. First-order spatial random coefficient non-negative integer-valued autoregressive (SRCINAR(1,1)) model.

- Communications in Statistics - Simulation and Computation*, 53(6):2662–2674, 2024. doi: 10.1080/03610918.2022.2083164.
- Christian H Weiß. Thinning operations for modeling time series of counts—a survey. *ASIA Advances in Statistical Analysis*, 92(3):319–341, 2008a. doi: 10.1007/s10182-008-0072-3.
- Christian H Weiß. The combined INAR(p) models for time series of counts. *Statistics & Probability Letters*, 78(13):1817–1822, 2008b. doi: 10.1016/j.spl.2008.01.036.
- Christian H Weiß. A new class of autoregressive models for time series of binomial counts. *Communications in Statistics - Theory and Methods*, 38(4):447–460, 2009. doi: 10.1080/03610920802233937.
- Christian H Weiß. *An Introduction to Discrete-Valued Time Series*. John Wiley & Sons, Ltd, 1st ed edition, 2018.
- Christian H Weiß, Fukang Zhu, and Hee-Young Kim. Tobit INARMA models for count time series with negative autocorrelation. *TEST*, 35(1): 117–156, 2026. doi: 10.1007/s11749-025-00994-6.
- P. Whittle. On stationary processes in the plane. *Biometrika*, 41(3–4):434–449, 1954. doi: 10.1093/biomet/41.3-4.434.
- Kai Yang, Mingming Jia, and Xiaogang Dong. An integer-valued spatial autoregressive model with application to covid-19 counts. *Journal of Applied Statistics*, 0(0):1–33, 2025. doi: 10.1080/02664763.2025.2565593.
- Rong Zhu and Harry Joe. A new type of discrete self-decomposability and its application to continuous-time Markov processes for modeling count data time series. *Stochastic Models*, 19(2):235–254, 2003. doi: 10.1081/STM-120020388.
- Rong Zhu and Harry Joe. Modelling count data time series with Markov processes based on binomial thinning. *Journal of Time Series Analysis*, 27(5):725–738, 2006. doi: 10.1111/j.1467-9892.2006.00485.x.

Appendix A. Derivations

Appendix A.1. Proof of Proposition 2.1.1

Let $\mathbf{Z}(s, t)$ denote all Bernoulli counting series involved in $X_{s,t}$ at “time” (s, t) . From the model recursion in (4), we see that $X_{s,t}$ can be understood as a function of $(\mathbf{D}_{s,t}, \varepsilon_{s,t}, \mathbf{Z}(s, t))$. Hence, we may write

$$\sigma(X_{s,t}, X_{s-1,t}, X_{s,t-1}, \dots) \subseteq \sigma(\mathbf{D}_{s,t}, \varepsilon_{s,t}, \mathbf{Z}(s, t), \mathbf{D}_{s-1,t}, \varepsilon_{s-1,t}, \mathbf{Z}(s-1, t), \dots),$$

where $\sigma(Y)$ denotes the σ -field generated by Y , and

$$\bigcap_{s=1}^{\infty} \bigcap_{t=1}^{\infty} \sigma(X_{s,t}, X_{s-1,t}, \dots) \subseteq \bigcap_{s=1}^{\infty} \bigcap_{t=1}^{\infty} \sigma(\mathbf{D}_{s,t}, \varepsilon_{s,t}, \mathbf{Z}(s, t), \mathbf{D}_{s-1,t}, \varepsilon_{s-1,t}, \mathbf{Z}(s-1, t), \dots).$$

The sequences $(\mathbf{D}_{s,t})$, $(\varepsilon_{s,t})$ and $(\mathbf{Z}(s, t))$ are i.i.d. as well as independent of each other by assumption, so $(\mathbf{D}_{s,t}, \varepsilon_{s,t}, \mathbf{Z}(s, t))$ is i.i.d. itself. Kolmogorov’s zero-one law (see, e.g., Billingsley, 1995, Theorem 22.3) gives that all events in this tail σ -field are trivial, i.e., every set in the tail σ -field has probability 0 or 1. Accordingly, the random field model $(X_{s,t})$ is ergodic and the proof of Proposition 2.1.1 is complete.

Appendix A.2. Proof of Proposition 2.1.2

If $(X_{s,t})$ is stationary, then the marginal pgf is given by

$$\begin{aligned} \text{pgf}_X(u) &= \mathbb{E}(u^{X_{s,t}}) = \mathbb{E}(\mathbb{E}(u^{X_{s,t}} | \mathbf{D}_{s,t})) = \sum_{(i,j) \in \mathcal{S}} \phi_{ij} \cdot \mathbb{E}(u^{\alpha \circ X_{s-t-j} + \varepsilon_{s,t}}) \\ &= \sum_{(i,j) \in \mathcal{S}} \phi_{ij} \cdot \text{pgf}_X(1 - \alpha + \alpha u) \cdot \text{pgf}_\varepsilon(u) = \text{pgf}_X(1 - \alpha + \alpha u) \cdot \text{pgf}_\varepsilon(u), \end{aligned}$$

as $(1 - \pi + \pi u)^n$ is the pgf of a binomially distributed random variable with parameters $n \in \mathbb{N}$ and $\pi \in (0, 1)$, and $\sum_{(i,j) \in \mathcal{S}} \phi_{ij} = 1$. Since the pgf captures the marginal distribution of the model and is identical to the pgf of the classical INAR(1) time series model, it follows that the CINAR’s mean and variance must also agree with those of the INAR(1) model. So the proof of Proposition 2.1.2 is complete.

Appendix A.3. Proof of Proposition 2.1.3

In order to derive the autocovariance function (ACvF) of the CINAR random field, we first consider mixed moments of the type $\mathbb{E}(X_{s,t} \cdot X_{s-k,t-l})$. Let $k \geq 1$ or $l \geq 1$. Then, the independence assumptions and application of Lemma 1 (i) of Silbernagel and Weiß (2026a) yield

$$\begin{aligned} \mathbb{E}(X_{s,t} \cdot X_{s-k,t-l}) &= \sum_{(i,j) \in \mathcal{S}} \phi_{ij} \cdot \mathbb{E}((\alpha \circ_{s,t} X_{s-i,t-j} + \varepsilon_{s,t}) \cdot X_{s-k,t-l}) \\ &= \mu_\varepsilon \cdot \mu_X + \sum_{(i,j) \in \mathcal{S}} \phi_{ij} \cdot \mathbb{E}((\alpha \circ_{s,t} X_{s-i,t-j}) \cdot X_{s-k,t-l}) = \mu_\varepsilon \cdot \mu_X + \alpha \sum_{(i,j) \in \mathcal{S}} \phi_{ij} \cdot \mathbb{E}(X_{s-i,t-j} \cdot X_{s-k,t-l}), \end{aligned}$$

because $(s-k, t-l)$ lies in the ‘‘past’’ of (s, t) . Furthermore, it holds that $\mathbb{E}(X_{s-i,t-j} \cdot X_{s-k,t-l}) = \gamma(k-i, l-j) + \mu_X^2$ and $\mu_\varepsilon = (1-\alpha)\mu_X$, so we obtain

$$\begin{aligned} \mathbb{E}(X_{s,t} \cdot X_{s-k,t-l}) &= (1-\alpha)\mu_X^2 + \alpha \sum_{(i,j) \in \mathcal{S}} \phi_{ij} \gamma(k-i, l-j) + \alpha \sum_{(i,j) \in \mathcal{S}} \phi_{ij} \mu_X^2 \\ &= \mu_X^2 + \alpha \sum_{(i,j) \in \mathcal{S}} \phi_{ij} \gamma(k-i, l-j) \quad \text{for } k \geq 1 \text{ or } l \geq 1. \end{aligned}$$

Analogously, for $k \leq -1$ or $l \leq -1$, we have

$$\begin{aligned} \mathbb{E}(X_{s,t} \cdot X_{s-k,t-l}) &= \mu_\varepsilon \mu_X + \sum_{(i,j) \in \mathcal{S}} \phi_{ij} \cdot \mathbb{E}(X_{s,t} \cdot (\alpha \circ_{s-k,t-l} X_{s-k-i,t-l-j})) \\ &= (1-\alpha)\mu_X^2 + \alpha \sum_{(i,j) \in \mathcal{S}} \phi_{ij} (\gamma(k+i, l+j) + \mu_X^2) \\ &= \mu_X^2 + \alpha \sum_{(i,j) \in \mathcal{S}} \phi_{ij} \gamma(k+i, l+j) \quad \text{for } k \leq -1 \text{ or } l \leq -1. \end{aligned}$$

All in all, the proof of Proposition 2.1.3 is complete.

Appendix A.4. Proof of Proposition 2.1.4

By the convolution formula and our independence assumptions, we have

$$\begin{aligned} \mathbb{P}(X_{s,t} = x | \mathcal{P}_{s,t}) &= \mathbb{P}\left(\sum_{(i,j) \in \mathcal{S}} D_{s,t;i,j} \cdot (\alpha \circ_{s,t} X_{s-i,t-j}) + \varepsilon_{s,t} = x | \mathcal{P}_{s,t}\right) \\ &= \sum_{y=0}^x \mathbb{P}(\varepsilon_{s,t} = y) \cdot \mathbb{P}\left(\sum_{(i,j) \in \mathcal{S}} D_{s,t;i,j} \cdot (\alpha \circ_{s,t} X_{s-i,t-j}) = x-y | \mathcal{P}_{s,t}\right) \\ &= \sum_{y=0}^x \mathbb{P}(\varepsilon_{s,t} = y) \cdot \sum_{(i,j) \in \mathcal{S}} \phi_{ij} \cdot \mathbb{P}(\alpha \circ_{s,t} X_{s-i,t-j} = x-y | X_{s-i,t-j}). \end{aligned}$$

The first claim follows from the fact that $\alpha \circ X_{s-i,t-j} | X_{s-i,t-j} \sim \text{Bin}(X_{s-i,t-j}, \alpha)$ is binomially distributed. Since $\varepsilon_{s,t}$ and $\mathbf{D}_{s,t}$ as well as the thinnings executed at ‘‘time’’ (s, t) are independent of the ‘‘past’’ $\mathcal{P}_{s,t}$, we have

$$\begin{aligned} \mathbb{E}(X_{s,t} | \mathcal{P}_{s,t}) &= \mathbb{E} \varepsilon_{s,t} + \sum_{(i,j) \in \mathcal{S}} \phi_{ij} \mathbb{E}(\alpha \circ_{s,t} X_{s-i,t-j} | \mathcal{P}_{s,t}) \\ &= \mu_\varepsilon + \sum_{(i,j) \in \mathcal{S}} \phi_{ij} \mathbb{E}(\alpha \circ_{s,t} X_{s-i,t-j} | X_{s-i,t-j}) = \mu_\varepsilon + \alpha \sum_{(i,j) \in \mathcal{S}} \phi_{ij} X_{s-i,t-j}. \end{aligned}$$

Concerning the conditional variance, it holds for the model definition in (4) that

$$\begin{aligned}\mathbb{V}(X_{s,t} | \mathcal{P}_{s,t}) &= \sum_{(i,j),(k,l) \in \mathcal{S}} \text{Cov}(D_{s,t;i,j} \cdot (\alpha \circ_{s,t} X_{s-i,t-j}), D_{s,t;k,l} \cdot (\alpha \circ_{s,t} X_{s-k,t-l}) | \mathcal{P}_{s,t}) \\ &\quad + 2 \sum_{(i,j) \in \mathcal{S}} \text{Cov}(D_{s,t;i,j} \cdot (\alpha \circ_{s,t} X_{s-i,t-j}), \varepsilon_{s,t} | \mathcal{P}_{s,t}) + \mathbb{V}(\varepsilon_{s,t} | \mathcal{P}_{s,t}).\end{aligned}$$

Due to the independence assumptions on $\varepsilon_{s,t}$, we have $\text{Cov}(D_{s,t;i,j} \cdot (\alpha \circ_{s,t} X_{s-i,t-j}), \varepsilon_{s,t} | \mathcal{P}_{s,t}) = 0$ and $\mathbb{V}(\varepsilon_{s,t} | \mathcal{P}_{s,t}) = \sigma_\varepsilon^2$, so it remains to consider the conditional covariances appearing in the first line. From the definition of the conditional covariance and the independence assumptions on $\mathbf{D}_{s,t}$, it follows that

$$\begin{aligned}\text{Cov}(D_{s,t;i,j} \cdot (\alpha \circ_{s,t} X_{s-i,t-j}), D_{s,t;k,l} \cdot (\alpha \circ_{s,t} X_{s-k,t-l}) | \mathcal{P}_{s,t}) \\ &= \mathbb{E}(D_{s,t;i,j} \cdot (\alpha \circ_{s,t} X_{s-i,t-j}) \cdot D_{s,t;k,l} \cdot (\alpha \circ_{s,t} X_{s-k,t-l}) | \mathcal{P}_{s,t}) \\ &\quad - \mathbb{E}(D_{s,t;i,j} \cdot (\alpha \circ_{s,t} X_{s-i,t-j}) | \mathcal{P}_{s,t}) \mathbb{E}(D_{s,t;k,l} \cdot (\alpha \circ_{s,t} X_{s-k,t-l}) | \mathcal{P}_{s,t}) \\ &= \mathbb{E}(D_{s,t;i,j} \cdot D_{s,t;k,l}) \cdot \mathbb{E}((\alpha \circ_{s,t} X_{s-i,t-j}) \cdot (\alpha \circ_{s,t} X_{s-k,t-l}) | \mathcal{P}_{s,t}) \\ &\quad - \mathbb{E}(D_{s,t;i,j}) \cdot \mathbb{E}(D_{s,t;k,l}) \cdot \mathbb{E}(\alpha \circ_{s,t} X_{s-i,t-j} | \mathcal{P}_{s,t}) \cdot \mathbb{E}(\alpha \circ_{s,t} X_{s-k,t-l} | \mathcal{P}_{s,t}).\end{aligned}$$

As only one component of $\mathbf{D}_{s,t}$ can equal 1 (and the remaining ones equal zero), $\mathbb{E}(D_{s,t;i,j} \cdot D_{s,t;k,l})$ equals ϕ_{ij} if $(i, j) = (k, l)$ and 0 otherwise. Therefore, we get

$$\text{Cov}(D_{s,t;i,j} \cdot (\alpha \circ_{s,t} X_{s-i,t-j}), D_{s,t;k,l} \cdot (\alpha \circ_{s,t} X_{s-k,t-l}) | \mathcal{P}_{s,t}) = \phi_{ij} \mathbb{E}((\alpha \circ_{s,t} X_{s-i,t-j})^2 | \mathcal{P}_{s,t}) \cdot \mathbb{1}_{\{(i,j)=(k,l)\}} - \phi_{ij} \phi_{kl} \alpha^2 X_{s-i,t-j} X_{s-k,t-l}.$$

Moreover, it holds that

$$\mathbb{E}((\alpha \circ_{s,t} X_{s-i,t-j})^2 | \mathcal{P}_{s,t}) = \mathbb{V}(\alpha \circ_{s,t} X_{s-i,t-j} | \mathcal{P}_{s,t}) + (\mathbb{E}(\alpha \circ_{s,t} X_{s-i,t-j} | \mathcal{P}_{s,t}))^2 = \alpha(1-\alpha)X_{s-i,t-j} + \alpha^2 X_{s-i,t-j}^2.$$

Summarizing everything, we obtain the desired result (11), and the proof of Proposition 2.1.4 is complete.

Appendix A.5. Proof of Equations (16)–(17)

By the convolution formula and our independence assumptions, we have

$$\begin{aligned}\mathbb{P}(Y_{u,v} = x | \mathcal{P}_{u,v}) &= \mathbb{P}\left(\sum_{(i,j) \in \mathcal{S}} D_{u,v;i,j} \cdot s(i, j) \cdot (\alpha \circ_{u,v} X_{u-i,v-j}) + \varepsilon_{u,v} = x | \mathcal{P}_{u,v}\right) \\ &= \sum_{y=0}^{\infty} \mathbb{P}(\varepsilon_{u,v} = y) \cdot \mathbb{P}\left(\sum_{(i,j) \in \mathcal{S}} D_{u,v;i,j} \cdot s(i, j) \cdot (\alpha \circ_{u,v} X_{u-i,v-j}) = x - y | \mathcal{P}_{u,v}\right) \\ &= \sum_{y=0}^{\infty} \mathbb{P}(\varepsilon_{u,v} = y) \cdot \sum_{(i,j) \in \mathcal{S}} \phi_{ij} \cdot \mathbb{P}(s(i, j) \cdot (\alpha \circ_{u,v} X_{u-i,v-j}) = x - y | X_{u-i,v-j}) \\ &= \sum_{y=0}^{\infty} \mathbb{P}(\varepsilon_{u,v} = y) \cdot \sum_{(i,j) \in \mathcal{S}} \phi_{ij} \cdot \mathbb{P}(\alpha \circ_{u,v} X_{u-i,v-j} = s(i, j) \cdot (x - y) | X_{u-i,v-j}).\end{aligned}$$

Here, $\alpha \circ_{u,v} X_{u-i,v-j} | X_{u-i,v-j} \sim \text{Bin}(X_{u-i,v-j}, \alpha)$ is binomially distributed, i.e., it has non-zero probability masses only if $s(i, j) \cdot (x - y) \in \{0, \dots, X_{u-i,v-j}\}$ such that the infinite sum $\sum_{y=0}^{\infty}$ always reduces to a finite one for each $(i, j) \in \mathcal{S}$.

Also note that $Y_{u,v}$ can only attain negative values if at least one $s(i, j) = -1$. Then, by the model recursion (15), the strongest negative value of $Y_{u,v}$ is attained if all positive summands are equal to zero, and if all negative summands become maximally negative. By the definition of binomial thinning, $\alpha \circ_{u,v} X_{u-i,v-j} \leq X_{u-i,v-j}$, so the strongest negative value of $Y_{u,v}$ is given by $L_{u,v} := \sum_{(i,j) \in \mathcal{S}} \min\{0, s(i, j)\} \cdot X_{u-i,v-j}$.

Finally, due to the relation $X_{u,v} = \max\{0, Y_{u,v}\}$, it holds that $X_{u,v}$ is equal to some truly positive value $x > 0$ iff $Y_{u,v} = x$. By contrast, any $Y_{u,v} \leq 0$ leads to $X_{u,v} = 0$. So

$$\mathbb{P}(X_{u,v} = 0 | \mathcal{P}_{u,v}) = \sum_{z=L_{u,v}}^0 \mathbb{P}(Y_{u,v} = z | \mathcal{P}_{u,v})$$

follows, and the proof of Equations (16)–(17) is complete.

Appendix B. Tabulated Simulation Results from Section 4

Table B.1: Mean and standard deviation of simulated estimates for Poi-CINAR(1, 1) random field, see Section 4.

Model $(\mu_\varepsilon, \theta_{01}, \theta_{10}, \theta_{11}) = (1, 0.1, 0.1, 0.1)$

	μ_ε	θ_{01}	θ_{10}	θ_{11}	μ_ε	θ_{01}	θ_{10}	θ_{11}	μ_ε	θ_{01}	θ_{10}	θ_{11}
Mean:	YW estimation				CLS estimation				CML estimation			
(10, 10)	1.067	0.086	0.085	0.080	1.006	0.096	0.097	0.101	0.999	0.097	0.099	0.102
(15, 15)	1.058	0.090	0.087	0.081	1.019	0.097	0.095	0.094	1.017	0.098	0.094	0.095
(20, 20)	1.041	0.091	0.092	0.088	1.014	0.097	0.098	0.098	1.010	0.097	0.099	0.098
(50, 50)	1.011	0.098	0.098	0.096	1.000	0.100	0.100	0.100	1.000	0.100	0.100	0.100
Std. dev.:	YW estimation				CLS estimation				CML estimation			
(10, 10)	0.203	0.081	0.081	0.075	0.230	0.093	0.092	0.095	0.219	0.093	0.094	0.093
(15, 15)	0.150	0.060	0.061	0.057	0.165	0.066	0.066	0.066	0.153	0.065	0.065	0.066
(20, 20)	0.124	0.049	0.050	0.048	0.132	0.052	0.053	0.053	0.124	0.051	0.052	0.052
(50, 50)	0.048	0.020	0.021	0.021	0.049	0.020	0.021	0.021	0.043	0.019	0.020	0.020

Model $(\mu_\varepsilon, \theta_{01}, \theta_{10}, \theta_{11}) = (1, 0.2, 0.2, 0.5)$

	μ_ε	θ_{01}	θ_{10}	θ_{11}	μ_ε	θ_{01}	θ_{10}	θ_{11}	μ_ε	θ_{01}	θ_{10}	θ_{11}
Mean:	YW estimation				CLS estimation				CML estimation			
(10, 10)	2.393	0.214	0.214	0.332	1.584	0.185	0.182	0.476	1.015	0.199	0.200	0.500
(15, 15)	1.809	0.217	0.217	0.384	1.313	0.188	0.190	0.490	1.009	0.198	0.199	0.502
(20, 20)	1.555	0.215	0.216	0.413	1.218	0.191	0.192	0.494	1.004	0.198	0.199	0.502
(50, 50)	1.168	0.211	0.209	0.464	1.042	0.199	0.197	0.499	1.004	0.201	0.199	0.500
Std. dev.:	YW estimation				CLS estimation				CML estimation			
(10, 10)	1.069	0.096	0.103	0.107	1.094	0.102	0.107	0.125	0.254	0.087	0.085	0.104
(15, 15)	0.714	0.069	0.070	0.076	0.728	0.069	0.071	0.082	0.157	0.049	0.052	0.060
(20, 20)	0.482	0.053	0.052	0.060	0.485	0.054	0.054	0.062	0.119	0.040	0.038	0.046
(50, 50)	0.182	0.020	0.021	0.024	0.183	0.021	0.021	0.025	0.044	0.014	0.014	0.018

Model $(\mu_\varepsilon, \theta_{01}, \theta_{10}, \theta_{11}) = (1, 0.3, 0.4, 0.1)$

	μ_ε	θ_{01}	θ_{10}	θ_{11}	μ_ε	θ_{01}	θ_{10}	θ_{11}	μ_ε	θ_{01}	θ_{10}	θ_{11}
Mean:	YW estimation				CLS estimation				CML estimation			
(10, 10)	1.592	0.261	0.345	0.074	1.333	0.260	0.357	0.114	1.017	0.293	0.393	0.110
(15, 15)	1.348	0.285	0.369	0.074	1.176	0.282	0.378	0.103	1.013	0.297	0.397	0.102
(20, 20)	1.228	0.294	0.383	0.077	1.090	0.291	0.391	0.099	1.009	0.298	0.399	0.100
(50, 50)	1.074	0.300	0.395	0.090	1.017	0.299	0.398	0.100	1.002	0.300	0.399	0.100
Std. dev.:	YW estimation				CLS estimation				CML estimation			
(10, 10)	0.627	0.106	0.103	0.078	0.656	0.115	0.115	0.106	0.253	0.095	0.095	0.094
(15, 15)	0.391	0.073	0.071	0.061	0.406	0.076	0.078	0.074	0.159	0.063	0.058	0.062
(20, 20)	0.276	0.055	0.053	0.051	0.279	0.059	0.057	0.059	0.119	0.044	0.045	0.048
(50, 50)	0.108	0.023	0.023	0.024	0.109	0.024	0.023	0.025	0.045	0.018	0.018	0.018

Table B.2: Mean and standard deviation of simulated estimates for NB-CINAR(1, 1) random field, see Section 4.

Model	$(\mu_\varepsilon, I_\varepsilon, \theta_{01}, \theta_{10}, \theta_{11}) = (1, 2, 0.1, 0.1, 0.1)$	μ_ε	I_ε	θ_{01}	θ_{10}	θ_{11}	μ_ε	I_ε	θ_{01}	θ_{10}	θ_{11}	μ_ε	I_ε	θ_{01}	θ_{10}	θ_{11}	
		YW estimation			CLS estimation			P-CML estimation			N-CML estimation						
Mean:		μ_ε	I_ε	θ_{01}	θ_{10}	θ_{11}	μ_ε	I_ε	θ_{01}	θ_{10}	θ_{11}	μ_ε	I_ε	θ_{01}	θ_{10}	θ_{11}	
(10, 10)		1.067	1.954	0.085	0.087	0.078	1.004	0.097	0.100	0.098	1.071	0.084	0.084	0.083	1.024	1.977	0.094
(15, 15)		1.053	1.961	0.088	0.089	0.084	1.012	0.095	0.096	0.097	1.060	0.086	0.085	0.085	1.012	1.991	0.094
(20, 20)		1.038	1.971	0.090	0.093	0.089	1.009	0.095	0.097	0.098	1.058	0.085	0.087	0.086	1.013	1.986	0.097
(50, 50)		1.014	1.990	0.097	0.098	0.096	1.003	0.099	0.100	0.100	1.051	0.089	0.090	0.088	1.002	1.996	0.100
Std. dev.:		YW estimation			CLS estimation			P-CML estimation			N-CML estimation						
(10, 10)		0.222	0.484	0.081	0.082	0.073	0.247	0.094	0.096	0.092	0.232	0.072	0.072	0.072	0.227	0.500	0.081
(15, 15)		0.170	0.315	0.063	0.063	0.060	0.183	0.068	0.069	0.069	0.162	0.051	0.052	0.052	0.155	0.314	0.058
(20, 20)		0.126	0.229	0.049	0.053	0.050	0.137	0.052	0.057	0.055	0.116	0.037	0.041	0.039	0.115	0.224	0.044
(50, 50)		0.053	0.099	0.022	0.021	0.021	0.054	0.023	0.021	0.022	0.045	0.015	0.015	0.015	0.043	0.087	0.017
Model	$(\mu_\varepsilon, I_\varepsilon, \theta_{01}, \theta_{10}, \theta_{11}) = (1, 2, 0.2, 0.2, 0.5)$	μ_ε	I_ε	θ_{01}	θ_{10}	θ_{11}	μ_ε	I_ε	θ_{01}	θ_{10}	θ_{11}	μ_ε	I_ε	θ_{01}	θ_{10}	θ_{11}	
		YW estimation			CLS estimation			P-CML estimation			N-CML estimation						
Mean:		μ_ε	I_ε	θ_{01}	θ_{10}	θ_{11}	μ_ε	I_ε	θ_{01}	θ_{10}	θ_{11}	μ_ε	I_ε	θ_{01}	θ_{10}	θ_{11}	
(10, 10)		2.395	1.676	0.215	0.208	0.333	1.562	0.182	0.178	0.479	1.353	0.190	0.188	0.483	1.048	1.907	0.197
(15, 15)		1.806	1.830	0.220	0.217	0.381	1.314	0.191	0.188	0.488	1.368	0.193	0.193	0.475	1.029	2.006	0.200
(20, 20)		1.555	1.845	0.216	0.215	0.413	1.218	0.192	0.191	0.495	1.338	0.191	0.192	0.480	1.011	1.993	0.198
(50, 50)		1.160	1.966	0.212	0.210	0.463	1.036	0.200	0.198	0.498	1.328	0.195	0.194	0.477	1.005	1.997	0.200
Std. dev.:		YW estimation			CLS estimation			P-CML estimation			N-CML estimation						
(10, 10)		1.128	0.899	0.106	0.102	0.110	1.148	0.111	0.104	0.128	0.413	0.082	0.080	0.095	0.296	0.634	0.083
(15, 15)		0.708	0.764	0.071	0.071	0.081	0.737	0.073	0.074	0.087	0.277	0.050	0.051	0.059	0.175	0.436	0.051
(20, 20)		0.484	0.618	0.051	0.053	0.061	0.503	0.051	0.053	0.064	0.200	0.035	0.036	0.042	0.124	0.306	0.036
(50, 50)		0.178	0.315	0.021	0.021	0.026	0.177	0.021	0.021	0.026	0.078	0.014	0.013	0.016	0.047	0.115	0.014

Table B.2 (cont.): Mean and standard deviation of simulated estimates for NB-CINAR(1, 1) random field, see Section 4.

Model $(\mu_\varepsilon, I_\varepsilon, \theta_{01}, \theta_{10}, \theta_{11}) = (1, 2, 0.3, 0.4, 0.1)$																		
	μ_ε	I_ε	θ_{01}	θ_{10}	θ_{11}	μ_ε	θ_{01}	θ_{10}	θ_{11}	μ_ε	θ_{01}	θ_{10}	θ_{11}					
Mean:	YW estimation					CLS estimation				P-CML estimation			N-CML estimation					
(10, 10)	1.579	1.753	0.265	0.341	0.076	1.337	0.261	0.352	0.118	1.371	0.270	0.356	0.098	1.065	1.946	0.292	0.386	0.107
(15, 15)	1.319	1.869	0.284	0.373	0.075	1.145	0.280	0.384	0.106	1.326	0.273	0.367	0.093	1.020	1.995	0.295	0.399	0.101
(20, 20)	1.212	1.930	0.293	0.390	0.072	1.079	0.291	0.396	0.095	1.305	0.276	0.371	0.091	1.010	1.987	0.299	0.401	0.097
(50, 50)	1.074	1.975	0.299	0.396	0.090	1.017	0.298	0.399	0.100	1.289	0.279	0.370	0.094	1.001	1.996	0.300	0.400	0.100
Std. dev.:	YW estimation					CLS estimation				P-CML estimation			N-CML estimation					
(10, 10)	0.646	0.734	0.107	0.107	0.079	0.664	0.117	0.124	0.108	0.431	0.092	0.091	0.081	0.333	0.653	0.093	0.093	0.085
(15, 15)	0.397	0.561	0.075	0.071	0.061	0.405	0.081	0.078	0.076	0.244	0.055	0.053	0.057	0.161	0.395	0.058	0.054	0.061
(20, 20)	0.286	0.464	0.057	0.057	0.052	0.290	0.060	0.061	0.059	0.183	0.042	0.042	0.042	0.123	0.279	0.044	0.043	0.045
(50, 50)	0.109	0.193	0.024	0.023	0.024	0.112	0.025	0.024	0.025	0.073	0.016	0.016	0.016	0.046	0.109	0.017	0.016	0.017

Table B.3: Mean and standard deviation of simulated estimates for Poi-CINAR(2, 2) random field, see Section 4.

Model $(\mu_\varepsilon, \theta_{01}, \theta_{02}, \theta_{10}, \theta_{11}, \theta_{12}, \theta_{20}, \theta_{21}, \theta_{22}) = (1, 0.1, \dots, 0.1)$

	μ_ε	θ_{01}	θ_{10}	θ_{11}	μ_ε	θ_{01}	θ_{02}	θ_{10}	θ_{11}	θ_{12}	θ_{20}	θ_{21}	θ_{22}
Mean:	CLS-1 estimation				CLS-2 estimation								
(10, 10)	3.009	0.133	0.134	0.128	1.308	0.089	0.090	0.088	0.089	0.101	0.085	0.097	0.097
(15, 15)	2.845	0.145	0.146	0.139	1.339	0.094	0.084	0.092	0.095	0.093	0.086	0.093	0.093
(20, 20)	2.665	0.160	0.161	0.146	1.214	0.096	0.094	0.098	0.095	0.096	0.090	0.095	0.095
(50, 50)	2.481	0.172	0.174	0.158	1.047	0.098	0.098	0.100	0.099	0.101	0.099	0.099	0.098
	CML-1 estimation				CML-2 estimation								
(10, 10)	2.526	0.165	0.170	0.157	1.026	0.097	0.100	0.098	0.098	0.105	0.094	0.101	0.100
(15, 15)	2.472	0.173	0.171	0.161	1.052	0.099	0.093	0.097	0.101	0.100	0.097	0.102	0.099
(20, 20)	2.356	0.182	0.182	0.165	1.023	0.101	0.100	0.100	0.100	0.100	0.096	0.098	0.099
(50, 50)	2.292	0.186	0.187	0.169	1.005	0.100	0.100	0.100	0.099	0.101	0.101	0.100	0.099
Std. dev.:	CLS-1 estimation				CLS-2 estimation								
(10, 10)	1.006	0.109	0.107	0.105	0.936	0.095	0.098	0.094	0.095	0.098	0.093	0.098	0.100
(15, 15)	0.773	0.082	0.082	0.085	0.716	0.073	0.067	0.071	0.075	0.073	0.069	0.069	0.075
(20, 20)	0.597	0.066	0.064	0.065	0.502	0.057	0.056	0.057	0.058	0.058	0.054	0.054	0.059
(50, 50)	0.245	0.027	0.027	0.027	0.185	0.023	0.022	0.023	0.023	0.023	0.022	0.023	0.024
	CML-1 estimation				CML-2 estimation								
(10, 10)	0.957	0.115	0.115	0.113	0.451	0.094	0.093	0.093	0.094	0.094	0.091	0.094	0.096
(15, 15)	0.658	0.080	0.078	0.081	0.280	0.064	0.059	0.062	0.065	0.063	0.060	0.061	0.066
(20, 20)	0.448	0.058	0.057	0.058	0.192	0.048	0.045	0.046	0.047	0.047	0.043	0.046	0.049
(50, 50)	0.170	0.022	0.022	0.022	0.065	0.018	0.016	0.017	0.018	0.017	0.016	0.017	0.017

Model $(\mu_\varepsilon, \theta_{01}, \theta_{02}, \theta_{10}, \theta_{11}, \theta_{12}, \theta_{20}, \theta_{21}, \theta_{22}) = (1, 0.15, 0.1, 0.15, 0.15, 0.05, 0.1, 0.05, 0.1)$

	μ_ε	θ_{01}	θ_{10}	θ_{11}	μ_ε	θ_{01}	θ_{02}	θ_{10}	θ_{11}	θ_{12}	θ_{20}	θ_{21}	θ_{22}
Mean:	CLS-1 estimation				CLS-2 estimation								
(10, 10)	3.217	0.172	0.176	0.172	1.490	0.124	0.081	0.126	0.128	0.070	0.085	0.070	0.093
(15, 15)	2.854	0.192	0.193	0.188	1.388	0.134	0.087	0.134	0.139	0.059	0.086	0.061	0.091
(20, 20)	2.666	0.202	0.200	0.197	1.271	0.142	0.088	0.140	0.147	0.054	0.091	0.053	0.093
(50, 50)	2.378	0.219	0.218	0.207	1.054	0.150	0.098	0.148	0.150	0.049	0.099	0.050	0.098
	CML-1 estimation				CML-2 estimation								
(10, 10)	2.383	0.215	0.221	0.207	1.032	0.143	0.094	0.143	0.143	0.066	0.095	0.066	0.095
(15, 15)	2.234	0.225	0.225	0.215	1.021	0.148	0.097	0.147	0.148	0.056	0.096	0.056	0.097
(20, 20)	2.181	0.228	0.228	0.217	1.023	0.150	0.097	0.149	0.153	0.050	0.099	0.049	0.099
(50, 50)	2.110	0.233	0.232	0.219	1.006	0.151	0.099	0.150	0.150	0.049	0.100	0.051	0.100
Std. dev.:	CLS-1 estimation				CLS-2 estimation								
(10, 10)	1.345	0.118	0.121	0.120	1.165	0.109	0.088	0.112	0.116	0.088	0.088	0.086	0.098
(15, 15)	0.942	0.088	0.090	0.088	0.838	0.083	0.069	0.082	0.083	0.062	0.068	0.062	0.073
(20, 20)	0.685	0.064	0.062	0.068	0.584	0.061	0.054	0.059	0.065	0.049	0.053	0.050	0.059
(50, 50)	0.279	0.028	0.026	0.028	0.211	0.025	0.023	0.024	0.026	0.023	0.022	0.024	0.025
	CML-1 estimation				CML-2 estimation								
(10, 10)	1.027	0.118	0.117	0.119	0.458	0.104	0.087	0.105	0.107	0.079	0.082	0.078	0.091
(15, 15)	0.592	0.077	0.077	0.079	0.252	0.067	0.057	0.068	0.068	0.053	0.058	0.054	0.064
(20, 20)	0.416	0.053	0.052	0.058	0.174	0.048	0.042	0.047	0.049	0.040	0.043	0.039	0.045
(50, 50)	0.161	0.020	0.020	0.022	0.063	0.018	0.016	0.017	0.018	0.016	0.016	0.016	0.017